

DIFFUSION OF GASES IN SOLIDS

—TRITIUM DIFFUSION IN REACTOR CLADDING MATERIALS
XENON DIFFUSION IN URANIUM DIOXIDE

P. M. ABRAHAM
JOHN AUSTIN
JOHN DAVIS
EUGENE DRISCOLL
KENNETH STARR

THOMAS ELLEMAN (Principal Investigator)
KURUYILLA VERGHESE

THIS DOCUMENT CONFIRMED AS
UNCLASSIFIED
DIVISION OF CLASSIFICATION
BY JH Kahn / amb
DATE 12/27/72

DEPARTMENT OF NUCLEAR ENGINEERING
North Carolina State University
Raleigh, North Carolina 27607

Period Covered:

November 1, 1971 to October 31, 1972

Prepared for the U. S. Atomic Energy Commission
under Contract No. AT-(40-1)-3508

R8116

NOTICE

This report was prepared as an account of work sponsored by the United States Government. Neither the United States nor the United States Atomic Energy Commission, nor any of their employees, nor any of their contractors, subcontractors, or their employees, makes any warranty, express or implied, or assumes any legal liability or responsibility for the accuracy, completeness or usefulness of any information, apparatus, product or process disclosed, or represents that its use would not infringe privately owned rights.

C 3296

MASTER

DEC 8 1972

DEC 8 1972

DISTRIBUTION OF THIS DOCUMENT IS UNLIMITED

peg

DISCLAIMER

This report was prepared as an account of work sponsored by an agency of the United States Government. Neither the United States Government nor any agency Thereof, nor any of their employees, makes any warranty, express or implied, or assumes any legal liability or responsibility for the accuracy, completeness, or usefulness of any information, apparatus, product, or process disclosed, or represents that its use would not infringe privately owned rights. Reference herein to any specific commercial product, process, or service by trade name, trademark, manufacturer, or otherwise does not necessarily constitute or imply its endorsement, recommendation, or favoring by the United States Government or any agency thereof. The views and opinions of authors expressed herein do not necessarily state or reflect those of the United States Government or any agency thereof.

DISCLAIMER

Portions of this document may be illegible in electronic image products. Images are produced from the best available original document.

DIFFUSION OF GASES IN SOLIDS

- Tritium Diffusion in Reactor Cladding Materials
- Xenon Diffusion in Uranium Dioxide

P. M. Abraham

John Austin

John Davis

Eugene Driscoll

Kenneth Starr

Thomas Elleman (Principal Investigator)

Kuruvilla Verghese

Department of Nuclear Engineering
North Carolina State University
Raleigh, North Carolina 27607

Period Covered:

November 1, 1971 to October 31, 1972

Prepared for the U. S. Atomic Energy Commission
under Contract No. AT-(40-1)-3508

MASTER

DISTRIBUTION OF THIS DOCUMENT IS UNLIMITED

This document is
PUBLICLY RELEASABLE
Larry E. Williams
Authorizing Official
Date: *05/24/2007*

89

TABLE OF CONTENTS

	Page
TRITIUM DIFFUSION IN TYPICAL REACTOR CLADDING MATERIALS	1
<u>ABSTRACT</u>	1
<u>INTRODUCTION</u>	3
<u>SUMMARY OF PREVIOUS WORK</u>	4
<u>CURRENT RESULTS</u>	7
I. Further Results on Surface Trapping in Austenitic Stainless Steels	7
II. Tritium Release from Zircaloy-2	8
III. A Calculation of Tritium Diffusion through Fuel Cladding	9
IV. Preliminary Results on Tritium Diffusion through ZrO ₂ Films on Zircaloy-2	15
V. Tritium Production in the Primary System of Pressurized Water Reactors	17
<u>DISCUSSION</u>	21
I. Diffusion in Stainless Steels and Zircaloy Samples	21
II. Tritium Release from Reactor Cladding	23
III. Tritium Production in PWR Coolant System	24
<u>CONCLUSIONS</u>	26
<u>REFERENCES</u>	27
 XENON DIFFUSION IN UO ₂	 43
<u>ABSTRACT</u>	43
<u>INTRODUCTION</u>	44
<u>SUMMARY OF PREVIOUS WORK</u>	45
<u>CURRENT RESULTS AND DISCUSSION</u>	53
<u>CONCLUSIONS</u>	57
<u>REFERENCES</u>	58

TRITIUM DIFFUSION IN REACTOR CLADDING MATERIALS

ABSTRACT

Analysis of tritium release data in Austenitic Stainless steels has revealed a significant amount of permanent trapping in the surface region. These data have been fitted to an existing trapping model to give values for the trapping parameters that obey the Arrhenius rate equation.

Gas release studies from Zircaloy-2 samples have been extended to the temperature range 25°C - 411°C and apparent diffusion coefficients in the surface region calculated. These coefficients are represented by

$$D = 0.12 \times 10^{-13} \exp \left[-5,500 \text{ Cal/RT} \right] \text{ cm}^2 \text{ sec}^{-1}$$

and are less than the bulk diffusion coefficients in Zircaloy-2 by a factor $10^7 - 10^8$.

A few measurements of tritium release from Zircaloy-2 samples which have known amounts of oxide on the surface have been conducted. The samples were oxidized for different times in 200 Torr pressure of oxygen at 500°C. The oxide thickness was measured by scanning electron microscopy. There is some indication that thick oxide layers ($> 0.2 \mu\text{m}$) do not provide any additional barrier against tritium release.

In order to assess the effects of surface regions with low diffusion coefficients on stainless steel and Zircaloy claddings on tritium release through the clad, a 3-region diffusion model of the cladding has been formulated, solved analytically and numerical results computed for typical PWR and BWR clad thicknesses. The computed release fractions are in good agreement with literature data from fuel pin irradiations.

A calculation of the tritium production in the primary coolant of the H. B. Robinson No. 2 PWR Plant at Hartsville, South Carolina has been performed. It shows that the tritium produced in the coolant can not fully account for all of the tritium found in measurements of the primary water at the plant, implying that tritium diffusion from the fuel to the coolant is a contributing source of tritium.

INTRODUCTION

Tritium diffusion studies in austenitic stainless steels and in Zircaloy-2 have been undertaken to assess the contribution made by ternary fission-produced tritium to activity in the primary coolant system in nuclear power reactors. Calculations of tritium diffusion through reactor cladding" based on bulk diffusion coefficients in these materials suggest that tritium release will be high. However, such predictions have been contradicted by preliminary observations in actual reactors which indicate that less than 0.1% of the ternary fission tritium diffuses through Zircaloy cladding.⁽²⁾ Previous results from the present research project⁽³⁾ have shown that a possible mechanism for this low release is tritium trapping in surface oxide layers resulting in apparent diffusion coefficients from the surface which are smaller than the bulk diffusion coefficient by a factor of $10^7 - 10^8$ in Zircaloy and about 10^2 in stainless steel.

This report reports on further results on surface trapping in stainless steel and Zircaloy-2 and a model that makes use of these results to predict an upper limit for the release of tritium from reactor cladding. A calculation of tritium activity in the primary coolant system of pressurized water reactors resulting from boron and lithium reactions is also presented and compared with actual plant data from an operating PWR. Some preliminary results on the behavior of tritium diffusion through ZrO_2 films on Zircaloy-2 are also reported.

SUMMARY OF PREVIOUS WORK

A detailed discussion of the tritium diffusion experiments and results has been reported in the past two annual reports and publications. These are:

Annual Program Reports: "Diffusion of Gases in Solids," USAEC

ORO-3508-6	11/69 to 10/70
ORO-3508-7	11/70 to 10/71

(Available from: Superintendent of Documents, U. S. Department of Commerce, Washington, D. C.)

"Diffusion of Tritium in Austenitic Stainless Steels," Jour. Nucl. Mat. 43, 119 (1972).

"Grain Boundary Diffusion of Tritium in 304- and 316-Stainless Steels," Jour. Nucl. Mat. (In Press).

"Tritium Diffusion in Zircaloy-2 and Stainless Steels," Trans. Amer. Nucl. Soc. 15, (1) 229 (1972).

A review of the major results presented in these publications are summarized here as background information.

1. Reproducible measurements of tritium concentration profiles resulting from diffusion in stainless steels and Zircaloy can be made by recoiling tritium into specimens through transmutation of a ${}^6\text{LiF}$ surface blanket, removing thin sections by electropolishing or chemical polishing, and assaying the polish solution for tritium after distillation.

2. Three components to the diffusion can be identified in stainless steel which involves trapping in the surface layers, bulk diffusion and grain boundary diffusion. The first two components are observed also in Zircaloy-2.

3. The bulk diffusion components in 304- and 316-stainless steels is consistent with classical diffusion solutions and Arrhenius plots of the diffusion coefficients yield straight lines. They are represented by

$$D = 0.018 \exp(-14,000 \text{ Cal/RT}) \text{ cm}^2\text{-sec}^{-1}$$

in stainless steels in the temperature range 25°C to 222°C and

$$D = 0.00021 \exp(-8500 \text{ Cal/RT}) \text{ cm}^2\text{-sec}^{-1}$$

in Zircaloy-2 in the temperature range -78°C to 204°C.

There was no apparent difference between 304- and 316-stainless steels, as expected.

4. The grain boundary diffusion coefficients in stainless steel were determined by a combination of sectioning using a lathe followed by electro-polishing to obtain the tritium profile to depths of the order of 2000 μm into the sample and fitting the data to Fisher's and Suzouka's model. The values obtained from the two models gave straight lines on the Arrhenius plots and agreed to within a factor 1.4. Fisher's model gave values represented by

G = grain boundary diffusion coefficient

$$= \exp(8.85 \pm 1.2) \exp(-0.45 \pm 0.03 \text{ eV/kT}) \text{ cm}^2\text{-sec}^{-1}$$

over the temperature range -78°C to 185°C. Only a relatively small fraction (of the order of 1-4%) of the injected tritium was found in the grain boundary diffusion component during the relatively short annealing times used in the experiment. These grain boundary diffusion coefficients are about 8 orders of magnitude greater than the bulk diffusion coefficient.

5. The near-surface trapping was studied by following the kinetics of tritium release from tritium doped specimens at constant temperature. It was shown that a two-region classical diffusion model which assumes a diffusion coefficient in the surface region which is different from the **bulk** diffusion coefficient could fit the surface release results although

the model did not explicitly account for tritium trapping and hence the observed buildup of tritium in the surface layers. The apparent diffusion coefficients for surface region determined by this model gave a linear Arrhenius plot for stainless steel, represented by

$$D = 0.00030 \exp (-15,400 \text{ Cal/RT}) \text{ cm}^2\text{-sec}^{-1}$$

in the temperature range 25° to 184°C . In the last annual report, there were only a few surface diffusion measurements for Zircaloy-2, but it was indicated that the surface diffusion coefficients were about 10^7 - 10^8 less than the bulk diffusion coefficients.

6. The surface trapping is believed to be associated with oxide films on the surface. However it is also conceivable that the helium which is injected to a depth of about $3 \mu\text{m}$ along with the tritium also could contribute to trapping through the generation of helium stabilized voids. This latter possibility was investigated by diffusing tritium through a layer of helium which was produced by prior implantation of monoenergetic helium ions into stainless steel foils. No trapping in the helium layer was observed.

7. The surface trapping effects could explain at least qualitatively the fact that tritium release rates from Zircaloy clad fuel elements is very low in contrast to the high release observed from stainless steel clad elements.

CURRENT RESULTS

Investigations in the past year included further tritium release studies on Zircaloy-2 and stainless steels, calculation of tritium in the primary coolant of pressurized water reactors, a calculation of tritium diffusion through reactor cladding using a 3-region classical diffusion model and some preliminary studies on tritium diffusion through ZrO_2 surface films on Zircaloy.

I. Further Results on Surface Trapping in Austenitic Stainless Steels

The previous annual report⁽³⁾ gave the Arrhenius plot of the apparent diffusion coefficient for tritium release from the surface region obtained by analysis of the gas release curves at short times using the two-region diffusion model. This model, however, would not be expected to fit the gas release kinetics at very long diffusion times if trapping plays a major role.

In order to better define the trap characteristics, tritium release measurements were made over long annealing times and the results are expressed in Figure 1. The curves indicate that the tritium release rate goes to zero after long diffusion times. The limiting release fraction is less than unity and increases with temperature. The saturation of these curves at values significantly below unity confirms trapping of some of the tritium atoms with no release from the traps. For the case of homogeneously distributed trapping sites with no release from the traps, Ong and Elleman⁽⁴⁾ have shown that the f vs $t^{\frac{1}{2}}$ curves should have a plateau with a limiting release fraction given by

$$f_1 = \frac{2}{R} (D/k_1)^{\frac{1}{2}}$$

where k_1 is the trapping rate constant. Assuming that this trapping model can be applied to the near surface region after long diffusion times, k_1 can be determined from the limiting fractional releases shown in Figure 1.

Figure 2 is an Arrhenius plot of the rate constant k_1 . Although there are only four data points to date, the data appear to fall on a straight line which can be represented by

$$k_1 = 160 \exp(-8,800 \text{ Cal/RT}) \text{ sec}^{-1}$$

over the temperature range 46°C to 180°C.

11. Tritium Release from Zircaloy-2

In the previous annual report⁽³⁾ it was shown that for three different temperatures at which diffusion was carried out, the tritium release from Zircaloy-2 was very small and the diffusion coefficient in the near surface region was about seven to eight orders of magnitude below the bulk diffusion coefficient.

To substantiate these findings over a broader temperature range, additional tritium release measurements in the temperature range 25°C to 411°C were carried out. The measurements were made by heating the samples in either a constant temperature oil bath or in a molten tin bath while flowing P-10 counting gas over the sample and measuring the activity of the flowing gas with a gas flow of proportional counter.

Figure 3 shows typical release curves from Zircaloy-2 samples. Less than 1% of the total tritium was released from all of the samples. Figure 4 gives the near-surface diffusion coefficient calculated from the two-region model.⁽³⁾ The gas release data have a fair degree of scatter but there is little doubt that the surface layers control the gas release

to give apparent diffusion coefficients which are less than the bulk diffusion coefficients by about a factor of $10^7 - 10^8$. The best fit of these apparent D values gives

$$D = 0.12 \times 10^{-13} \exp \left[5500 \text{ Cal/RT} \right] \text{ cm}^2\text{sec}^{-1}$$

111. A calculation of Tritium Diffusion through Fuel Cladding

Calculation of tritium diffusion through claddings typically treats the clad as a single homogeneous region. From the diffusion data presented here and in the earlier report⁽³⁾ it would appear that the diffusion rate limiting regions are the surfaces and therefore a more realistic representation of the clad should provide for:

- a) an inner oxidized region in contact with the fuel,
- b) a middle region of normal bulk material, and
- c) an outer region also composed of an oxidized layer.

The surface regions in an actual cladding would change with the operation of the reactor and are therefore difficult to characterize. The objective of the calculation presented here is to predict an upper limit for the tritium release from reactor cladding with simple oxide surfaces and apparent diffusion coefficients identical to those measured in the present study. At least in the case of BWR cladding, it is known that the surfaces of the Zircaloy tubing are oxidized to thicknesses of the order of $1-3 \mu\text{m}$,⁽⁴⁾ during fuel element manufacture.

The geometry assumed in this calculation is shown in Figure 5. Transport of tritium is believed to be by diffusion in UO_2 followed by release into the fuel-clad gap. The tritium is then absorbed on the inner wall of the cladding and diffuses through the three regions of the cladding. The following assumptions are made in developing the mathematical model:

1. The residence time of tritium in the gas plenum is short compared to the diffusion times; so that tritium released from the fuel is very quickly absorbed on the cladding surface. This assumption is justified by the observations in actual fuel pin irradiations by Goode and Cox,⁽⁵⁾ Melehan⁽⁶⁾ and by Grossman and Hegland⁽⁷⁾ which show undetectable or negligible amounts of tritium in the gas plenum. Furthermore, this assumption would tend to give an upper limit for the amount released from the clad surface.

2. Tritium arriving at the outer surface of the cladding is released immediately into the coolant. This assumption is made because there is insufficient data available now to enable a rigorous treatment of the sorption and desorption behavior of tritium at the clad-coolant interface. This assumption is also conservative since it will give high values for the release of tritium into the coolant.

3. Diffusion is assumed to occur at the average clad temperature in the radial direction. Diffusion in the axial direction is neglected since the temperature gradient in the axial direction is much smaller than in the radial direction.

With the above assumptions, the boundary value problem for the three-region system may be formulated as

$$D_1 \frac{\partial^2}{\partial x^2} C_1(x, t) = \frac{d}{dt} C_1(x, t) \quad , \quad -x_1 \leq x \leq 0$$

$$D_2 \frac{\partial^2}{\partial x^2} C_2(x, t) = \frac{d}{dt} C_2(x, t) \quad , \quad 0 \leq x \leq x_2$$

$$D_3 \frac{\partial^2}{\partial x^2} C_3(x, t) = \frac{d}{dt} C_3(x, t) \quad , \quad x_2 \leq x \leq x_3$$

with the boundary conditions

$$C_3(x_3, t) = 0$$

$$C_1(0, t) = C_2(0, t)$$

$$C_2(x_2, t) = C_3(x_2, t)$$

$$D_1 \frac{\partial}{\partial x} C_1(x, t) \Big|_{x=0} = D_2 \frac{\partial}{\partial x} C_2(x, t) \Big|_{x=0}$$

$$D_2 \frac{\partial}{\partial x} C_2(x, t) \Big|_{x=x_2} = D_3 \frac{\partial}{\partial x} C_3(x, t) \Big|_{x=x_2}$$

and
$$J(t) = D_1 \frac{\partial}{\partial x} C_1(x, t) \Big|_{x=0}$$

where the D 's and C 's are diffusion coefficients and tritium concentrations in each region. $J(t)$ is the source current of tritium from the fuel and is calculated from a boundary value problem for the fuel region. The initial conditions are

$$C_1(x, 0) = C_2(x, 0) = C_3(x, 0) = 0$$

The solution of the above boundary value problem is complicated by the inhomogeneous boundary condition at the inner surface of the cladding. It can be deduced, however, from the solution for similar heat conduction equations given by **Ölcer**⁽⁸⁾ and is given by

$$C_i(x, t) = \sum_{v=1}^{\infty} C_{iv} \phi_{iv}(x) \phi_{1v}(-x_1) J'(\lambda_v, t) \quad (1)$$

where
$$\frac{1}{C_v} = \sum_{i=1}^3 \int_{R_i} \phi_{iv}^2(x) dx \quad (2)$$

$$J'(\lambda_{i\nu}, t) = e^{-\lambda_{i\nu} t} \int_0^t e^{\lambda_{i\nu} \tau} J(\tau) d\tau \quad (3)$$

and the λ 's and $\phi_{i\nu}$'s are the eigen values and eigen functions of the associated homogeneous boundary value problem. Omitting the arbitrary amplitude, the eigen functions are:

$$\left. \begin{aligned} \phi_{1\nu}(x) &= \cos(\beta_{1\nu} x) - \tan(\beta_{1\nu} x_1) \sin(\beta_{1\nu} x) \\ \phi_{2\nu}(x) &= \cos(\beta_{2\nu} x) - \sqrt{\frac{D_1}{D_2}} \tan(\beta_{1\nu} x_1) \sin(\beta_{2\nu} x) \\ \phi_{3\nu}(x) &= G_{1\nu} \left[\sin(\beta_{3\nu} x) - \tan(\beta_{3\nu} x_3) \cos(\beta_{3\nu} x) \right] \end{aligned} \right\} \quad (4)$$

where

$$G_{1\nu} = \frac{\cos(\beta_{2\nu} x_2) - \sqrt{\frac{D_1}{D_2}} \tan(\beta_{1\nu} x_1) \sin(\beta_{2\nu} x_2)}{\sin(\beta_{3\nu} x_2) - \tan(\beta_{3\nu} x_3) \cos(\beta_{3\nu} x_2)} \quad (5)$$

Since, $\lambda_{i\nu} = D_i \beta_{i\nu}^2$, the eigen values may be determined from the transcendental equation:

$$\begin{aligned} &\sqrt{\frac{D_1}{D_2}} \tan(\beta_{1\nu} x_1) \tan(\beta_{2\nu} x_2) + \sqrt{\frac{D_2}{D_3}} \tan(\beta_{2\nu} x_2) \tan\{\beta_{3\nu}(x_3 - x_2)\} \\ &+ \sqrt{\frac{D_1}{D_3}} \tan(\beta_{1\nu} x_1) \tan\{\beta_{3\nu}(x_3 - x_2)\} - 1 = 0 \end{aligned} \quad (6)$$

Substituting the eigen functions given by Eq. (4) into Eq. (2), we have

$$\frac{1}{c_{i\nu}} = I_{C1} + I_{C2} + I_{C3} \quad (7)$$

where

$$I_{C1} = \frac{1}{2\beta_{1\nu}} \left[\beta_{1\nu} x_1 \sec^2(\beta_{1\nu} x_1) + \tan(\beta_{1\nu} x_1) \right]$$

$$\begin{aligned}
&= \frac{1}{2\beta_{2v}} \left[\beta_{2v} x_2 \left\{ 1 + \frac{D_1}{D_2} \tan^2(\beta_{1v} x_1) \right\} + \frac{\sin(2\beta_{2v} x_2)}{2} \left\{ 1 - \frac{D_1}{D_2} \tan^2(\beta_{1v} x_1) \right\} \right. \\
&\quad \left. + \sqrt{\frac{D_1}{D_2}} \tan(\beta_{1v} x_1) \left\{ \cos(2\beta_{2v} x_2) - 1 \right\} \right] \quad (8)
\end{aligned}$$

and

$$I_{C3} = \frac{G_{1v}^2}{2\beta_{3v}} \sec^2(\beta_{3v} x_3) \left[\beta_{3v} (x_3 - x_2) - \frac{\sin\{2\beta_{3v} (x_3 - x_2)\}}{2} \right]$$

The amount of diffusing species released per unit surface area of the slab over time t is given by the time integral of the current into the slab minus the total amount remaining inside the clad. Therefore,

$$N(t) = \int_0^t J(t) dt - \sum_{i=1}^3 \int_{R_i} C_i(x, t) dx \quad (9)$$

where $C_i(x, t)$ is given by Eq. (1).

In order to determine $J(t)$, it is necessary to solve another boundary value problem for the release of tritium from a cylindrical fuel rod.

Assuming radial diffusion only and uniform generation of tritium in the **fuel rod, the system of equations for classical diffusion in a rod with a volumetric production rate A_o is**

$$D \nabla_r^2 C(r, t) + A_o = \frac{\partial C}{\partial t} (r, t)$$

$$C(a, t) = 0, \quad C(r, 0) = 0, \quad 0 \leq r \leq a$$

and $C(0, t)$ is finite.

D is the tritium diffusion coefficient in the fuel and C is the concentration in the fuel. It can be shown that the fraction of the diffusing

tritium released from a cylindrical rod in time t is given by

$$f_{UO_2}(t) = 1 - \frac{2}{\pi} \left[\frac{a^2}{16} - 2 \sum_{m=1}^{\infty} \frac{e^{-\alpha_m^2 t}}{\alpha_m^4} \right] \quad (10)$$

where α_m 's are the zeros of the zero-order Bessel Function $J_0\left(\frac{a}{m}\right)$ and a is the radius of the fuel rod. The current $J(t)$ leaving the surface of the fuel and entering the cladding is given by

$$J(t) = \frac{A a}{2} \left[1 - 4 \sum_{m=1}^{\infty} \frac{e^{-E_m t}}{\gamma_m} \right] \quad (11)$$

where $\gamma_m = a \alpha_m$

and $E_m = \gamma_m^2 \frac{D}{a^2}$

Substituting Eq. (11) into (3), and using Eqs. (1), (4), (7), and (9), it can be shown that the fission product tritium that is released from the cladding is given by

$$f(t) = f_{UO_2}(t) - \sum_{v=1}^{\infty} C_{v,v} P_v F(\lambda_v, t) \quad (12)$$

where

$$P_v = \sec(\beta_{1v} x_1) \left[\frac{\tan(\beta_{1v} x_1)}{\beta_{1v}} + \frac{\sin(\beta_{2v} x_2) + \frac{D_1}{D_2} \tan(\beta_{1v} x_1) \{\cos(\beta_{2v} x_2) - 1\}}{\beta_{2v}} + \frac{G_{1v} \{\cos[\beta_{3v}(x_3 - x_2)] - 1\}}{\beta_{3v} \cos(\beta_{3v} x_3)} \right] \quad (13)$$

and

$$F(\lambda_v, t) = \frac{1 - e^{-\lambda_v t}}{\lambda_v t} + 4 \sum_{m=1}^{\infty} \frac{e^{-E_m t} - e^{-\lambda_v t}}{\gamma_m^2 (E_m - \lambda_v) t} \quad (14)$$

The solution from this model has been programmed for numerical calculations. The diffusion coefficient in the fuel was obtained by fitting Eq. (10) to the data of Grossman and Hegland⁽⁷⁾ for their CP-206 fuel rod. Figure 6 shows the fraction of the total fission product tritium that is released from the cladding surface into the coolant at any time t for a total clad of thickness $814 \mu\text{m}$ which is typical of the thickness of BWR cladding. The curve labeled 1 is the fraction released from the fuel surface; curves 2 and 3 are for clads without any surface films. Curve 4 is for the case of $2 \mu\text{m}$ thick surface layers on either side of a bulk diffusion region. The values of diffusion coefficients are approximately those of stainless steel at about 300°C . Curve 5 is for a similar case with the surface region diffusion coefficient lower than the bulk diffusion coefficient by a factor 10^6 . Figure 7 shows corresponding results for a total clad thickness of $617 \mu\text{m}$ which is typical for PWR fuel elements. Figure 8 gives similar results for 814 and $617 \mu\text{m}$ thick clads for the case where the diffusion coefficients in the surface differ by a factor of 10^8 from the bulk diffusion coefficient. This case approximates Zircaloy cladding at about 300°C . The implication of these curves is discussed in Section II of the Discussion.

IV. Preliminary Results on Tritium Diffusion through ZrO_2 Films on Zircaloy-2

The results so far have shown that oxide films on Zircaloy-2 tend to be excellent barriers against tritium diffusion. All these studies were carried out with samples where very thin oxygen layers were formed during the course of the experiment. In order to determine the diffusion-limiting characteristics of thicker oxide layers on Zircaloy, an investigation has been started on the effect of surface film thickness on tritium transport. The preliminary results from this study are reported below.

An experimental system as shown in Figure 9 has been set up to strain-anneal Zircaloy specimens under vacuum, to oxidize the specimens at a constant temperature and oxygen pressure and to monitor the tritium release from the tritium-doped samples during their diffusion anneal. The process of strain annealing and oxidation are straight-forward. Oxidation is carried out simultaneously on a 0.5" diacylindrical sample and on a 10-mil foil. The foil sample is used for determining the oxide thickness and the gas release measurement is carried out using the cylindrical sample. For the diffusion anneal, P-10 counting gas is passed over a sheet of Zircaloy-2 placed in the furnace tube to remove any residual moisture and then over the tritium-doped sample. At the exit of the furnace, this sweep gas is mixed with a small amount of neutral hydrogen and this mixture is passed through a gas-flow proportional counter. The hydrogen is added to minimize absorption of tritium on the counter walls which would lead to erroneous counts. The background minimizing effect of hydrogen was checked by exiting the sweep gas before it reached the counter, flushing the counter with fresh P-10 gas, and checking the background count rate in the counter.

Four samples of Zircaloy-2 were oxidized at 500°C and 200 Torr oxygen pressure for 10 minutes, (2 samples), and 50 minutes and 100 minutes. The foil specimens were cut in two, polished to remove surface deformation and the oxide films observed in a scanning electron microscope. Figure 10 shows three such scanning electron micrographs. The thickness of the oxide regions can be measured from the micrographs and converted to a density thickness using the known microscope magnification and the conversion factor quoted by Gulbransen and Andrew.⁽⁹⁾ These values may be compared with the values of Kofstad⁽¹⁰⁾ and Figure 11 shows that they agree reasonably well.

Table I gives the apparent diffusion coefficient for surface release as obtained from the gas release studies on samples with different oxide

thicknesses. All of the release measurements were carried out at 380°C after oxidation at 500°C and 200 Torr oxygen pressure.

Table I. Apparent D for Zircaloy-2 with different thicknesses of oxide films on the surface

Sample Number	Weight Gain (mg/cm ²)	Thickness (SEM)	Oxidation Time Min.	D Apparent (cm ² /sec)
10	0.07	0.2 μm	10	1.255 x 10 ⁻¹⁷
5	0.14	0.3 - 0.6 μm	50	8,729 x 10 ⁻¹⁵
9	0.18	0.7 μm	100	2.313 x 10 ⁻¹⁶
12	0.14	0.65 μm	50	4.555 x 10 ⁻¹⁶

These data are preliminary and the studies are continuing.

V. Tritium Production in the Primary System of Pressurized Water Reactors

Tritium is produced in a pressurized water reactor primary coolant system by a variety of sources in addition to possible diffusion of fission product tritium. In the H. B. Robinson # 2 Plant of the Carolina Power and Light Company (739 MWe PWR), the monitored activity in the primary system ranges from about 0.1 to 0.2 μc/cm³. In order to assess what fraction of this tritium could be accounted for by transmutation reactions in the water and what fraction by clad diffusion, a calculation has been performed using the H. B. Robinson Plant data on boron and lithium and the primary system. Earlier work of a similar nature by Ray⁽¹⁾ drastically overestimates the tritium production rate in primary coolant, since he did not consider lithium control in the primary system.

In addition to ternary fission and burnable poison rods, the following sources of ^3H exist in PWR's:

1. $^{10}\text{B}(n, 2\alpha) ^3\text{H}$ is the boron shim.
2. $^7\text{Li}(n, n\alpha) ^3\text{H}$ in Li used for pH control.
3. $^6\text{Li}(n, \alpha) ^3\text{H}$ in Li used for pH control.
4. $^{10}\text{B}(n, \alpha) ^7\text{Li}(n, n\alpha) ^3\text{H}$

The first two reactions dominate the transmutation produced ^3H in the primary system because the low abundance of ^6Li in natural lithium minimizes the contribution from reaction (3) and because most of the ^7Li produced from ^{10}B is removed by lithium removal systems in order to maintain the concentration at about 2 ppm for pH control. This fact also makes it unnecessary to consider the fourth reaction.

The $^{10}\text{B}(n, 2\alpha) ^3\text{H}$ reaction has a threshold energy of about 1 MeV and its cross-section may be approximated by a linear function increasing from 15 mb at 1 MeV to 75 mb at 5 MeV and a constant at 75 mb from 5 MeV to 10 MeV.

The $^7\text{Li}(n, n\alpha) ^3\text{H}$ reaction cross-section increases approximately linearly from zero at 3 MeV to 400 mb at 6 MeV and remains constant at 400 mb from 6 MeV to 10 MeV. The production rate of ^3H in Ci/day, from these two reactions can be calculated from the equation

$$\rho V_c^{-1} N(t) = 1.31 \times 10^6 N_B(t) \int_1^{10} \sigma_B(E) \phi(E) dE + 1.01 \times 10^7 N_L(t) \int_1^{10} \sigma_L(E) \phi(E) dE \quad (15)$$

where $N(t)$ = production rate of tritium in Ci/day at time t .

ρ, V_c = density (g-cm^{-3}) and volume (cm^3) of the coolant.

$N_B(t)$ = natural boron concentration (ppm) in the coolant at time t .

$N_L(t)$ = lithium-7 concentration (ppm) at time t .

$\sigma(E)$ = energy-dependent reaction cross-sections (cm^2).

and $\phi(E)$ = energy-dependent neutron flux between 1 and 10 MeV ($\text{n cm}^{-2} \text{sec}^{-1}$).

The total amount of tritium, $T(t)$, in the coolant in curies at time t can be shown to be given by

$$T(t) = T_0 + \left\{ \int_{t_0}^t \dot{N}(t') \exp \left[\int_{t_0}^{t'} F(t'') dt'' \right] dt' \right\} \exp \left[- \int_{t_0}^t F(t') dt' \right] \quad (16)$$

where T_0 = curies of tritium present initially at time t_0 .

t = time in days.,

F = dilution factor [i.e., the fraction of primary coolant volume turned over daily] in day^{-1} .

Using the Watt fission spectrum given by

$$\phi(E) dE = 0.453 A_N e^{-1.036E} \text{Sinh} (2.29E)^{\frac{1}{2}} dE$$

and a value of the total flux above 1 MeV usually obtained from Safety Analysis Report for a nuclear plant [typically $6 \times 10^{13} \text{ n cm}^{-2} \text{ sec}^{-1}$ for a 1000 MWe PWR⁽¹²⁾], the normalizing factor A_N is determined. The daily boron and lithium concentrations are available from plant data. Thus, equations (15) and (16) may be used in short time steps to compute the tritium concentration in the primary system at any time during the plant operation and compared against the tritium activity monitored at the plant.

Assuming a linear decrease in boron concentration [i.e., $N_B(t) = a + bt$] with time and a constant value of lithium concentration, and dilution factor, it can be shown that the tritium activity at time t is given by

$$N(t) \text{ Ci/day} = \frac{V \rho}{F} \left\{ 1.31 \times 10^6 \sigma_1 \left[\left(a - \frac{\rho}{F} \right) (1 - e^{-Ft}) + bt \right] + 1.01 \times 10^7 N_L \sigma_2 (1 - e^{-Ft}) \right\} \quad (17)$$

where
$$\sigma_1 = \int_1^{10} \sigma_B(E) \phi(E) dE \quad (18)$$

and
$$\sigma_2 = \int_1^{10} \sigma_L(E) \phi(E) dE \quad (19)$$

Equations (16) and (17) have been programmed to calculate the tritium production for a typical 1000 MWe PWR with the following parameters:

$$V_c = 650 \text{ ft}^3$$

$$\rho = 0.7 \text{ g cm}^{-3}$$

$$F = 0.2\%$$

$$N_L = 2 \text{ ppm}$$

$$a = 1500 \text{ ppm}$$

$$b = -3 \text{ ppm day}^{-1}$$

W, the total water volume = 9500 ft³.

Figure 12 shows the total tritium in the coolant produced from the ¹⁰B and ⁷Li reactions for the above set of parameters. The major contribution is from the ¹⁰B(n,2α)³H reaction. Figure 13 shows the effect of the dilution factor on the tritium concentration.

Using Equations (15) and (16), a computer program was developed to evaluate the tritium activity in the primary coolant system resulting from the boron and lithium reactions in the H. B. Robinson # 2 PWR Plant. Actual day-to-day plant data on boron and lithium were used in the computations, for a total of 80 days of operation. The computed concentration after the 80 days was 0.091 μc/cm³ as compared to the value of 0.18 μc/cm³ from assay of the coolant water. Thus, approximately half of the total tritium in the primary system could be accounted for by the ¹⁰B(n,2α)³H and ⁷Li(n,nα)³H reactions, with the remainder presumably due to diffusion of ternary fission tritium through the clad.

DISCUSSION

I. Diffusion in Stainless Steel and Zircaloy Samples

The trapping constant k shown as a function of $\frac{1}{T}$ in Figure 2 appears to obey the Arrhenius rate equation based on the four data points. It can be shown that

$$k = \frac{3D}{L^2}$$

where L is the diffusion length for trapping. Since the activation energy for diffusion in the near-surface region is greater than the activation energy associated with k , it would appear that L^2 will increase with increase in temperature, thereby lowering the amount of trapping.

The extensive set of degassing experiments performed on Zircaloy-2 confirms the existence of a near-surface trapping effect. Less than 1% of the contained tritium was released even at temperatures as high as 411°C and heating times of several hours. The surface layer diffusion coefficients are typically eight orders of magnitude below the bulk diffusion coefficients. Figure 14 shows the comparison of bulk diffusion coefficients and the surface diffusion coefficients from the present work against past results reported in literature. Most of the work was done on Zirconium; of these the only other measurement on Zircaloy-2 are by Sawatzky⁽¹³⁾ whose results are represented by the curve labelled (1) and by Kearns⁽¹⁴⁾ in curve (2). Within error limits, the measured activation energy for the present work and Sawatzky's results agree well, but the absolute values are an order of magnitude higher than in the present work. Most of the past results shown in Figure 14 are for hydrogen diffusion in Zirconium. The curves labelled (3), (4) and (5) were obtained respectively by Schwartz and Mallet⁽¹⁵⁾, Mallet and Albrecht⁽¹⁶⁾ and Someno⁽¹⁷⁾ by forming a hydride layer on Zirconium followed by matching layers off the specimens and hydrogen analysis

of the layers. These curves were all extrapolated to temperatures below the range of actual measurement which makes comparison of these results with the present work not very reliable. Curve (6) was obtained by Cupp and Elubacher⁽¹⁸⁾ through an autoradiographic technique of obtaining tritium concentration gradients in the temperature range 149°C to 240°C. Their absolute values as well as the activation energy of 9070 Cal/mole compare favorably with the present work. Curve (7) was obtained by Gulbransen and Andrew⁽¹⁷⁾ using a weight gain method following permeation of hydrogen over 60°C to 250°C range of temperature and are the lowest values reported in literature. This technique is susceptible to surface films influencing the results which might explain the low values reported. Curve (8) is obtained from the work of Mallet and Albrecht⁽¹⁵⁾ and are degasing coefficients measured over the interval 635°C to 800°C. Their significantly higher values over the degasing coefficients reported in the present work may reflect ineffectiveness of the oxide surface to retain hydrogen at high temperatures. The activation energy from the degasing data of Mallet and Albrecht is about four times higher than that obtained in the present work. It is interesting that Smith⁽¹⁸⁾ has observed a factor of four increase in activation energy for hydrogen permeation through oxide films in going from low temperature (< 500°C) permeation studies to high temperature (~ 700°C) measurements.

The preliminary results reported in this work on oxide films on Zircaloy-2 indicate that the oxide thickness measured by scanning electron microscopy is consistent with the weight gain curves reported by Kofstad⁽¹⁰⁾. However, the surface layer diffusion coefficients obtained for various oxide thicknesses vary over three orders of magnitude.

Dawson, et al.,⁽²⁰⁾ have shown that the oxidation proceeds initially at a parabolic rate with time, then goes into a cubic dependence on time and at longer times the time dependence becomes linear. The above authors believe that the transition from parabolic to cubic is a result of the onset

of crack formation in the oxide. As oxidation progresses, the oxide layers tend to become porous. The oxidation of Sample # 10 was completed in the parabolic (non-porous) region. It is interesting to note that it had the lowest measured surface diffusion coefficient ($5 \times 10^{-18} \text{ cm}^2 \text{ sec}^{-1}$) which is two orders of magnitude less than the value at 380°C shown in Figure 4. With the other samples for which reliable surface release data are available, (see Table 1), the oxidation took place either in cubic region or in the parabolic-cubic transition and therefore would be expected to have a more porous oxide layer than Sample # 10. These samples did release a much larger amount of tritium than Sample # 10 and had degasing coefficients which are not significantly less than the values at 380°C in Figure 4. It thus appears that homogeneous oxide layers formed by oxidation in the linear region may provide effective tritium barriers on Zircaloy and become less effective when cracks or porosity develop. However, more extensive measurements must be carried out in order to confirm this.

II. Tritium Release from Reactor Cladding

The results of the 3-region model calculation of tritium diffusion through the cladding is expected to give an upper limit for the amount released from the cladding surface into the primary coolant.

It is evident that in the case of stainless steel cladding, a year of operation results in release of approximately 70 - 80% of the total tritium produced in the fuel for typical light water cladding thicknesses. This is consistent with the observation by Laconte and Malinowski⁽²¹⁾ that in Core I of the Connecticut Yankee reactor, over 60% of the tritium produced in the core was released through the cladding. Steele⁽²²⁾ also reported that from 50 - 90% of the generated tritium escaped from the stainless steel clad rods of the Lacrosse Boiling Water Reactor.

In the case of Zircaloy clad fuel pins, it is evident from Figures 6, 7, and 8 that much less than 1% release of the tritium will be expected based on diffusion through the bulk and surface regions. This is consistent with the results of Goode and Cox⁽⁵⁾ who reported that for lowpower-rated Zircaloy clad fuel rods, there was apparently no loss of tritium from the rod. Melehan^(6,23) also found that Little or no tritium was released from Zircaloy cladding.

It should be emphasized that the low tritium release predicted for Zircaloy is due exclusively to the low surface layer permeability for tritium and is not a consequence of the bulk diffusion properties of the alloy. A more accurate prediction of tritium release from the cladding would be more complex than the treatment presented with the 3-region model. Short circuit paths such as grainboundaries and dislocations might increase the release over what is calculated here, while various surface effects such as adsorption and desorption, hydride formation, etc., could tend to further retard the tritium release from the surface,

III. Tritium Production in PWR Coolant System

The results of the calculation of tritium from boron and lithium reactions show that the earlier calculations by Ray⁽¹¹⁾ overestimates the amount of tritium produced in PWR's by more than an order of magnitude. The discrepancy is because the major contribution in Ray's results arise from $^{10}\text{B}(n,\alpha)^7\text{Li}(n,n\alpha)^3\text{H}$ reaction. In present day PWR's lithium concentration is controlled to about 2 ppm and ^7Li is not allowed to build up with the reactor as assumed by Ray. As a result, the major contribution to tritium generation in the primary coolant comes from the $^{10}\text{B}(n,2\alpha)^3\text{H}$ reaction.

The calculations on the Robinson # 2 Plant shows that approximately half of the monitored tritium activity can be accounted for by boron and

lithium reactions. There are various possible explanations for the balance, The ternary fission tritium production in the core over a year's operation amounts to 8180 curies⁽²⁴⁾. Over the period in which the calculations were made, the equivalent amount would be approximately 2600 curies, If one assumes that 0.6 percent of this tritium diffused through the Zircaloy cladding, which is reasonable from the 3-region calculations presented earlier, it would result in an additional concentration of about $0.05 \mu\text{c cm}^{-3}$ in the primary water. This alone would be sufficient to account for most of the difference between the monitored tritium activity and the calculated value. In addition, there could be release from the pyrex burnable poison rods which also have Zircaloy cladding. The tritium production in the poison rods is estimated to be about 1700 curies/year so that this is not expected to be a major source of tritium release into the coolant.

Thus it appears that the tritium levels observed in the H. B. Robinson Plant is consistent with what is to be expected from boron and lithium reactions in the coolant and diffusion of ternary fission tritium through the cladding.

CONCLUSIONS

1. Measurement of the surface layer diffusion coefficients in Zircaloy-2 are shown to be about 10^8 less than the bulk diffusion coefficient and are represented by the Arrhenius expression

$$D = 0.12 \times 10^{-13} \exp - (5500 \text{ Cal/RT}) \text{ cm}^2 \text{ sec}^{-1}$$

over the temperature range of 25°C to 411°C.

2. Preliminary results on oxide growth and tritium release through oxide layers in Zircaloy-2 indicate that high temperature oxidation of the surface resulting in thickness greater than 0.2 μm does not significantly decrease the release of tritium.
3. Calculation of tritium diffusion through stainless steel and Zircaloy cladding using a 3-region model give calculated release fractions which are consistent with the tritium release reported in actual fuel pin irradiations.
4. Tritium concentrations measured in the H. B. Robinson # 2 PWR primary system can be essentially accounted for by the $^{10}\text{B}(n, 2\alpha) ^3\text{H}$ and $^7\text{Li}(n, n\alpha) ^3\text{H}$ reactions and by tritium diffusion through Zircaloy cladding.

REFERENCES

1. Ray, J. W., R. O. Wooten and R. H. Barnes, "Investigation of Tritium Generation and Release in B Power Plants," USAEC Report BMI-1787 (1966).
2. Jacobs, D. G., "Sources of Tritium and Its Behavior Upon Release to the Environment," USAEC Report TID-24635 (1968).
3. Austin, J. H., R. D. Calder, J. C. Carter, T. S. Elleman and K. Verghese, "Diffusion of Gases in Solids," USAEC Report ORO-3508-7 (1971).
4. Private communication with the staff of GE Fuel Fabrication Plant, Wilmington, North Carolina, October 6 (1972).
5. Goode, J. H. and C. M. Cox, "The Distribution of Fission Product Tritium in a Zircaloy-clad UO_2 Blanket Rod from PWR-1," USAEC Report ORNL-TM-2994 (1970).
6. Melehan, J. B., "Tritium Content of a Yankee Core \bar{V} Zircaloy-clad UO_2 Fuel Rod," USAEC Report E-IT-70-208 (1970).
7. Grossman, L. N. and J. O. Hegland, "Tritium Distribution in High Power Zircaloy Fuel Elements," USAEC Report GEAP-12205 (1971).
8. Ölcner, N. Y., "Theory of Unsteady Heat Conduction in Multicomponent Finite Regions," Ingenieur. Archiv. 36:285-293 (1968).
9. Gulbransen, E. A. and K. F. Andrew, "Reaction of Hydrogen with Pre-oxidized Zircaloy-2 at 300' to 400°C, Jour. Electrochem. Society 104, 709-712 (1957).
10. Kofstad, Per, "High Temperature Oxidation of Metals," John Wiley and Sons, New York (1966).
11. Ray, J. W., "Tritium in Power Reactors," Reactor and Fuel-Processing Technology 12, No. 1, 19-26, Winter 1968-69.
12. Reference Safety Analysis Report, RESAR, Vol. 2, Table 14, 22, Westinghouse Electric Corporation, (1970).
13. Sawatzky, A., The Diffusion and Solubility of Hydrogen in the Alpha-phase of Zircaloy-2, Jour. Nucl. Mat. 2, 62-68 (1960).
14. Kearns, J. J., Diffusion Coefficient of Hydrogen in Alpha Zirconium, Zircaloy-2 and Zircaloy-4, Jour, Nucl. Mat, 43:330-338 (1972).
15. Schwartz, C. M. and M. W. Mallett, Observations on the Behavior of Hydrogen and Zirconium, Trans. ASM 46, 641-654 (1954).
16. Mallet, M. W. and W. M. Albrecht, Low-pressure Solubility and Diffusion of Hydrogen in Zirconium, Jour. Electrochem. Soc. 104, 142-146 (1957).

17. Someno, M., Solubility and Diffusion of Hydrogen in Zirconium, Nippon Kinzoku Gakkaishi 24, 249-253 (1960).
18. Gulbransen, E. A, and K. F. Andrew, Diffusion of Hydrogen and Deuterium in High-Density Zirconium, Jour. Electrochem, Soc. 101, 560-566 (1954).
19. Smith, T., Kinetics and Mechanism of Hydrogen Permeation of Oxide Films on Zirconium, Jour. Nucl. Mat, 18, 323-336 (1966).
20. Dawson, J. K., G. Long, W. E. Seddon and J. F. White, "The Kinetics and Mechanism of the Oxidation of Zircaloy at 350°C - 500°C," Jour. Nucl. Mat, 25, 179-200 (1968).
21. Laconte, J. and D. D. Malinowski, "Tritium in Pressurized Water Reactors," Paper presented at the Tritium Symposium, Las Vegas, Nevada, August 30 - September 2 (1971).
22. Steele, T. A., "Tritium Generation and Release to In-plant and Off-site Environs of the Lacrosse Boiling Water Reactor," Paper presented at the Tritium Symposium, Las Vegas, Nevada, August 30 - September 2 (1971).
23. Melehan, J. B., "Analysis of Tritium Retention in High Power Saxton and CVTR Fuel," USAEC Report E-IT-71-51, Westinghouse Electric Corporation, Pittsburgh, Pennsylvania, U. S. A.
24. Final Safety Analysis Report, H. B. Robinson # 2 Plant, Vol. 3, Table 9.2.6.

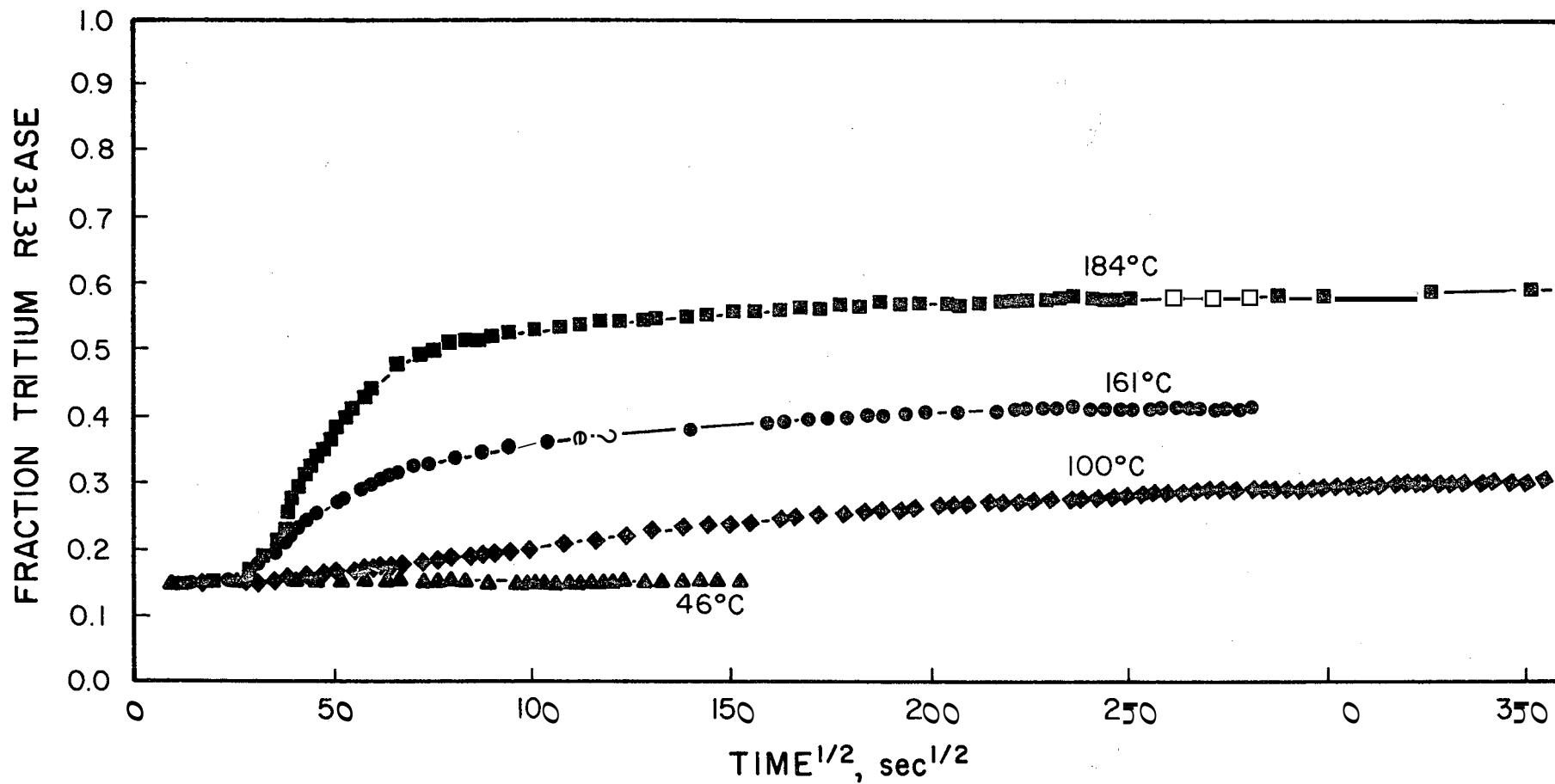


Figure 1. Tritium fraction released from recoil-doped stainless steel samples at four different temperatures as a function of (time)^{1/2}

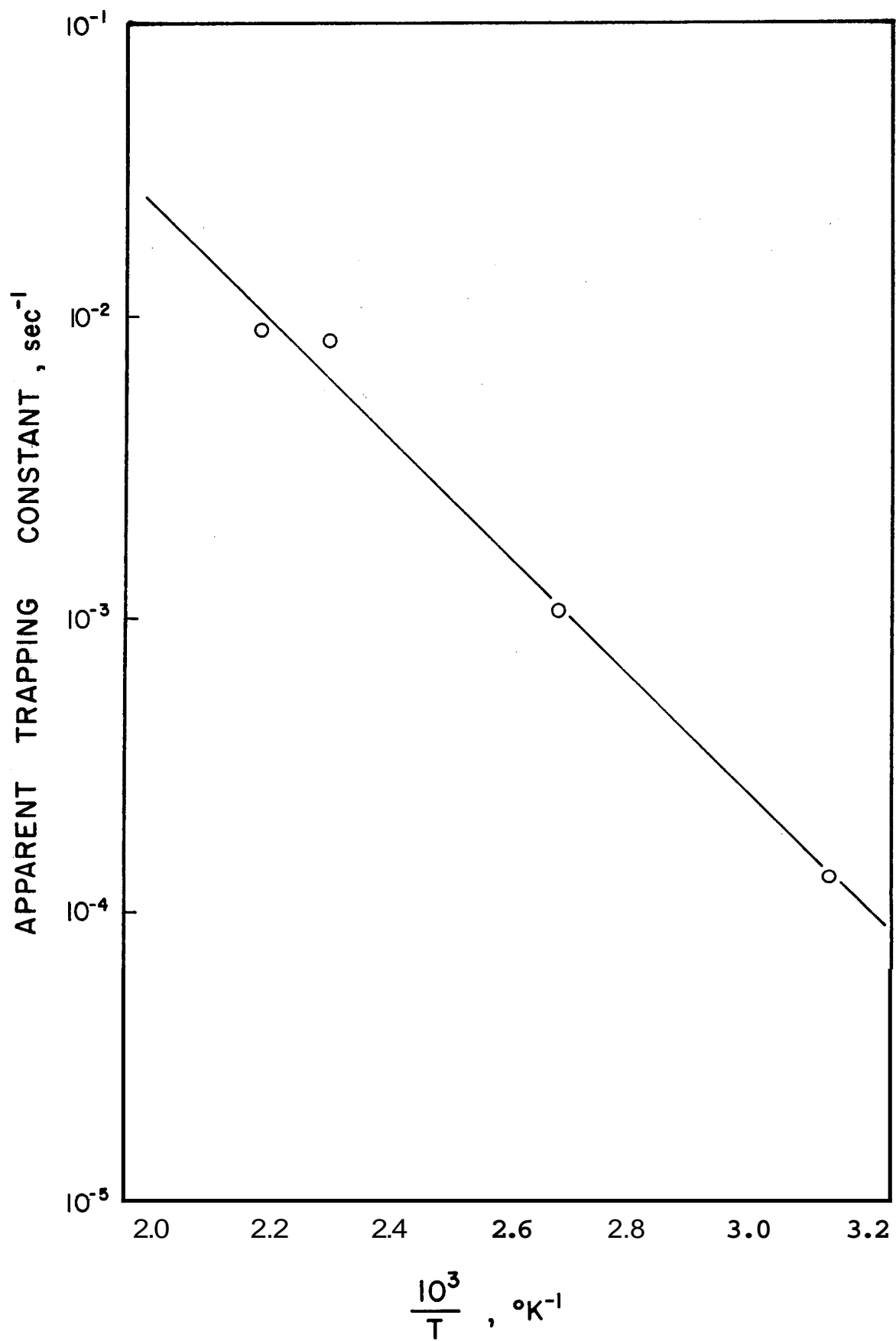


Figure 2. Arrhenius plot of trapping rate constant k

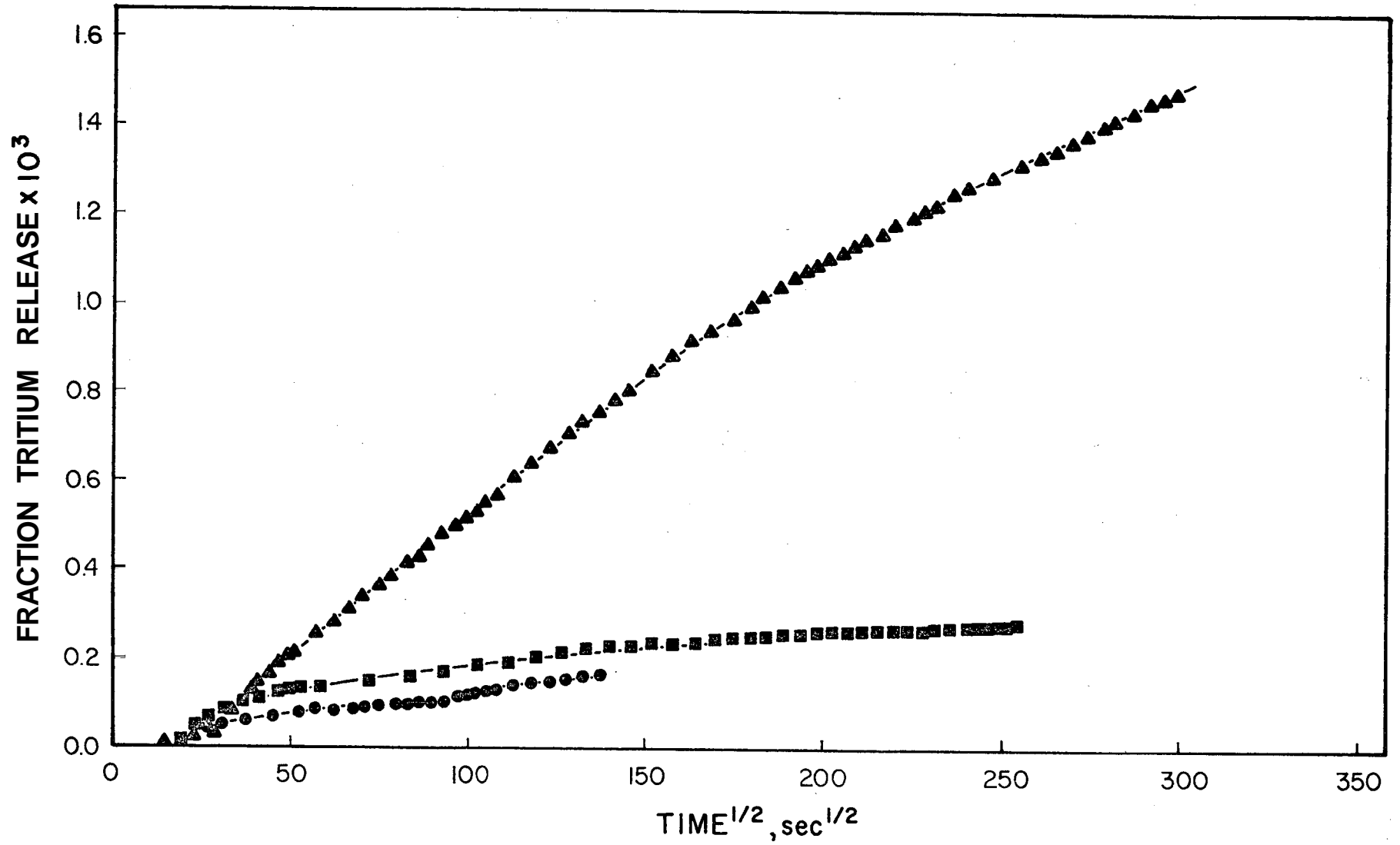


Figure 3. Fractional release of tritium from Zircaloy-2 samples

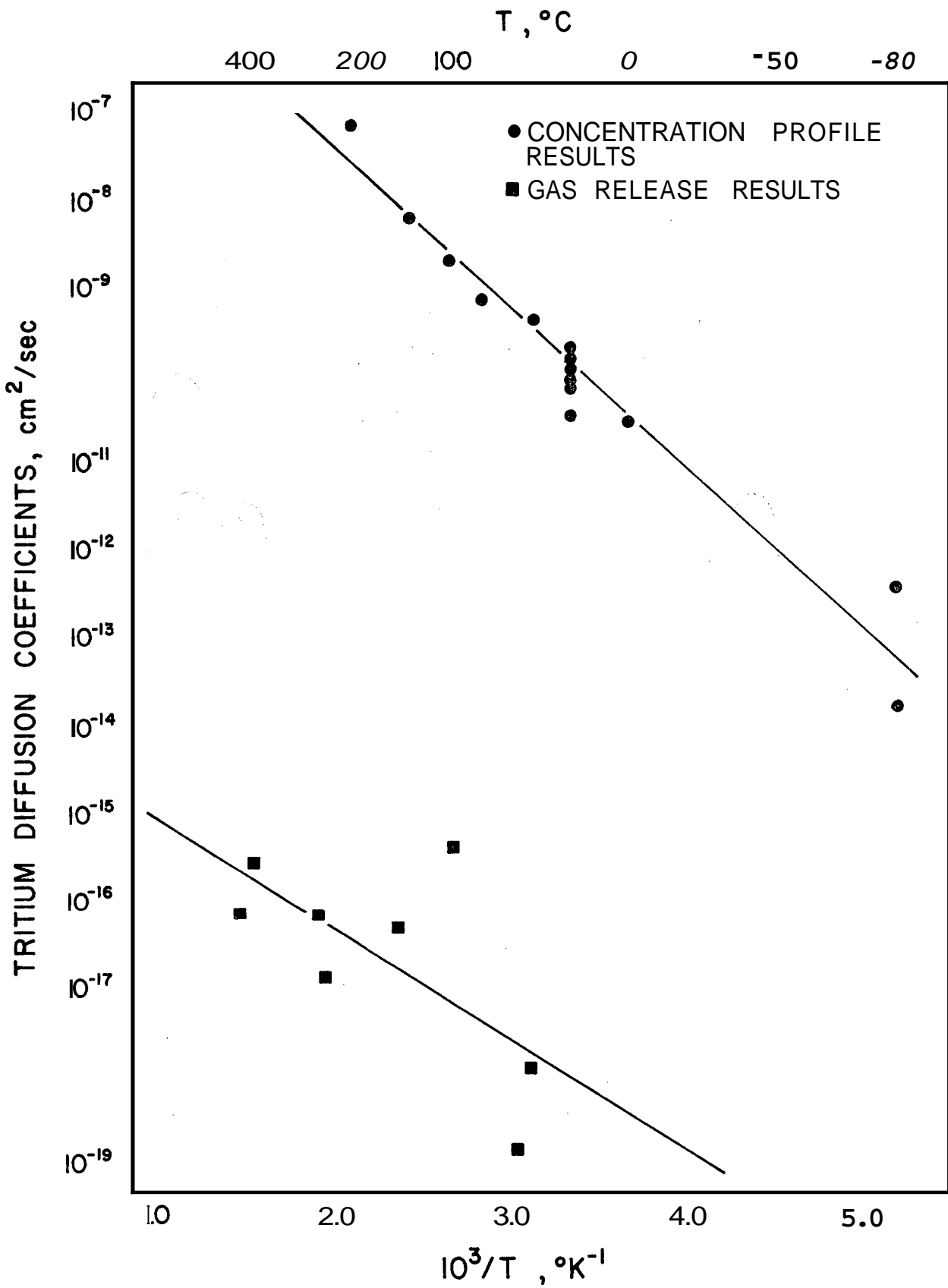


Figure 4. Arrhenius plot of bulk diffusion coefficients and surface region diffusion coefficients in Zircaloy-2

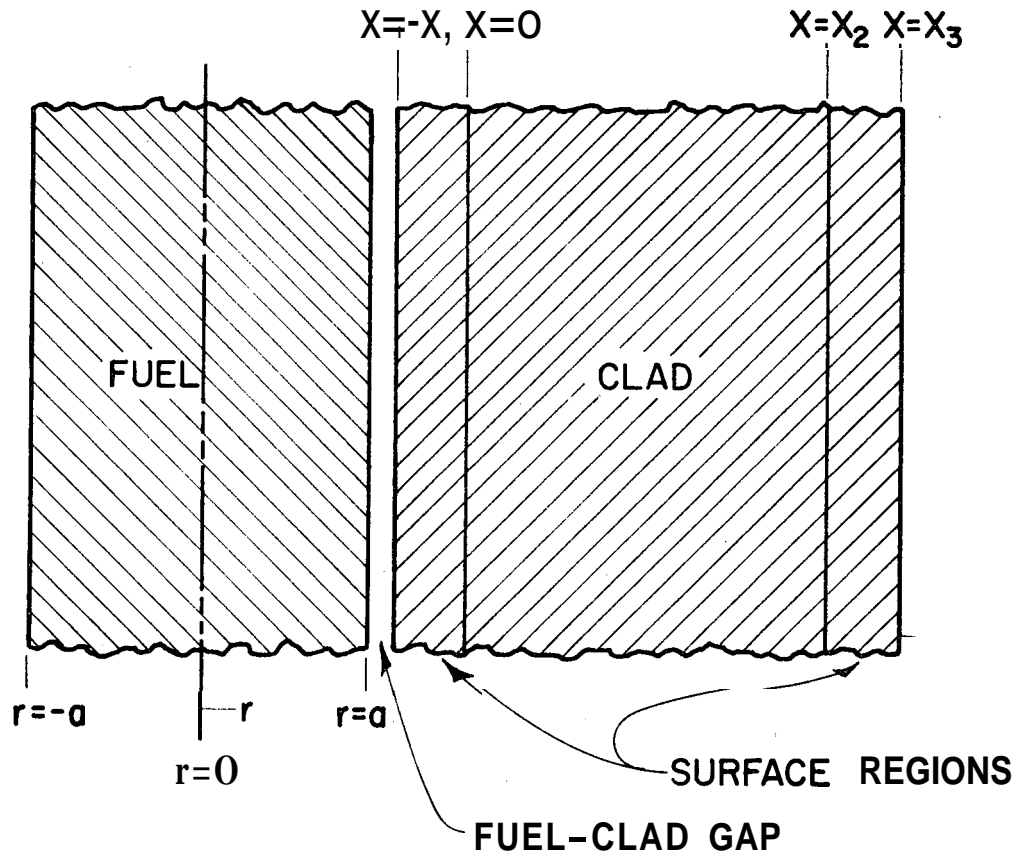


Figure 5. Fuel element configurations used for the 3-region diffusion model

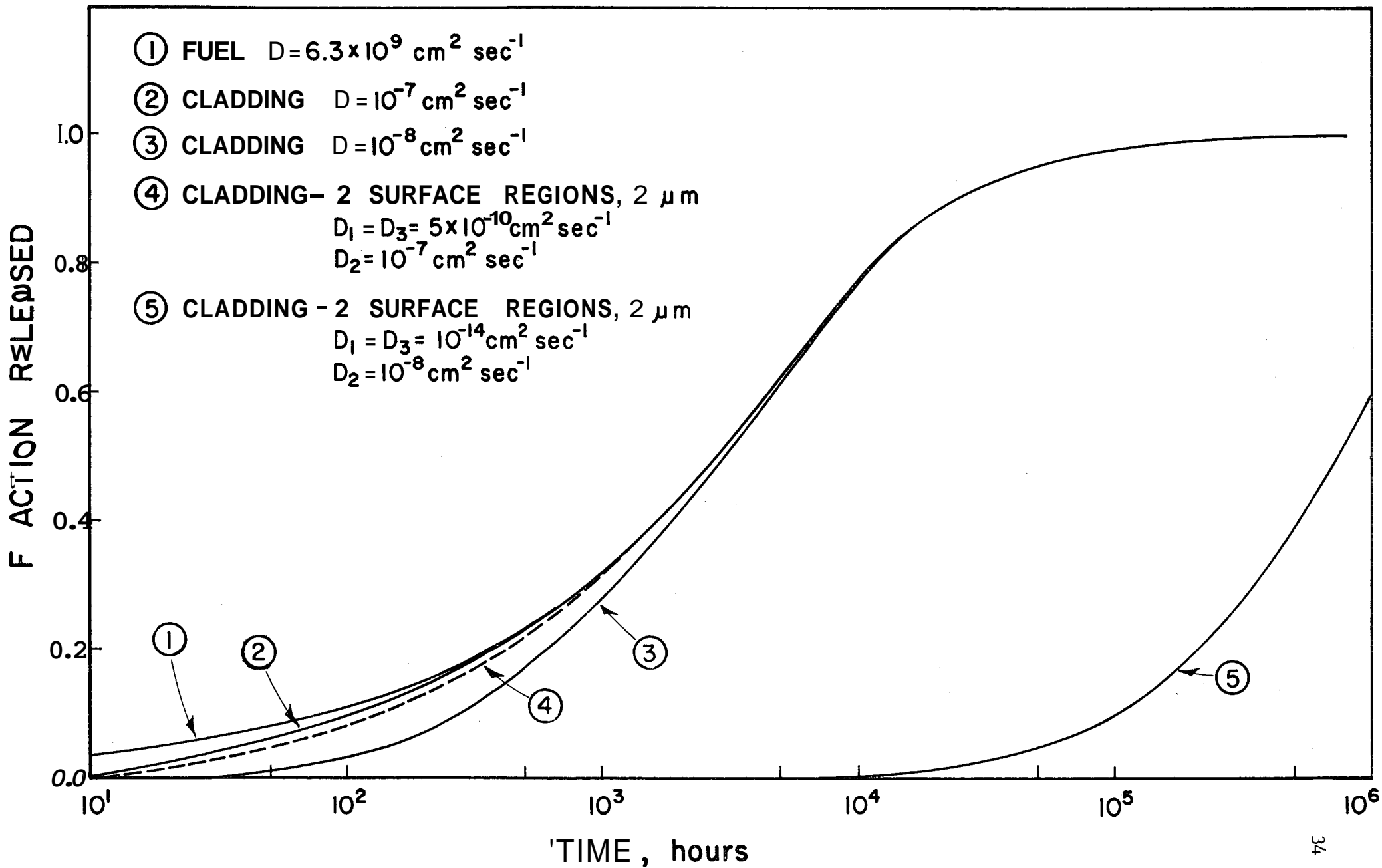


Figure 6. Calculated fractional release of tritium for a fuel pin with 814 μm thick cladding

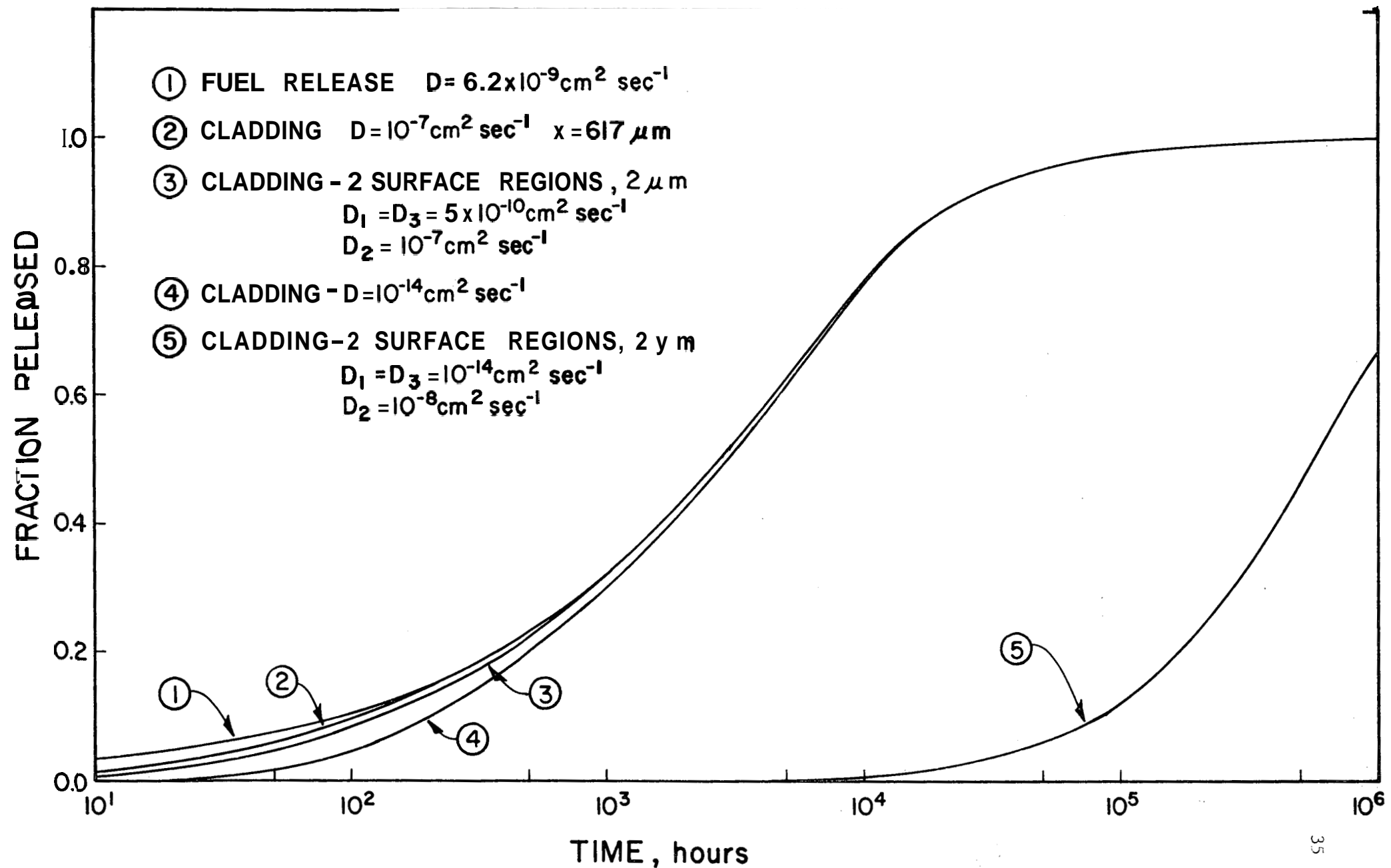


Figure 7. Calculated fractional release of tritium for a fuel pin with 617 μm thick cladding

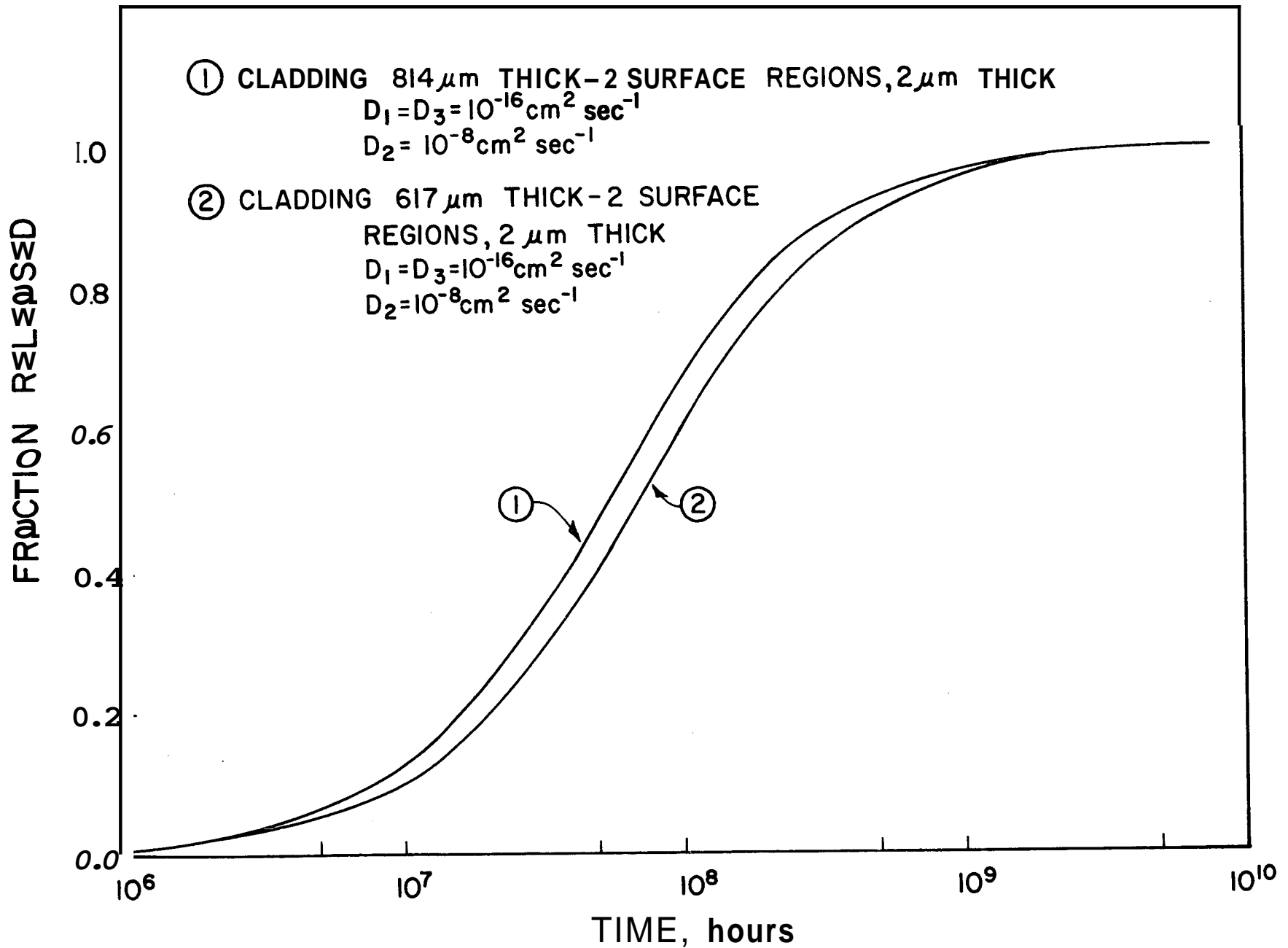


Figure 8. Calculated fractional release from claddings where the surface region D is smaller than the bulk D by a factor of 10^8

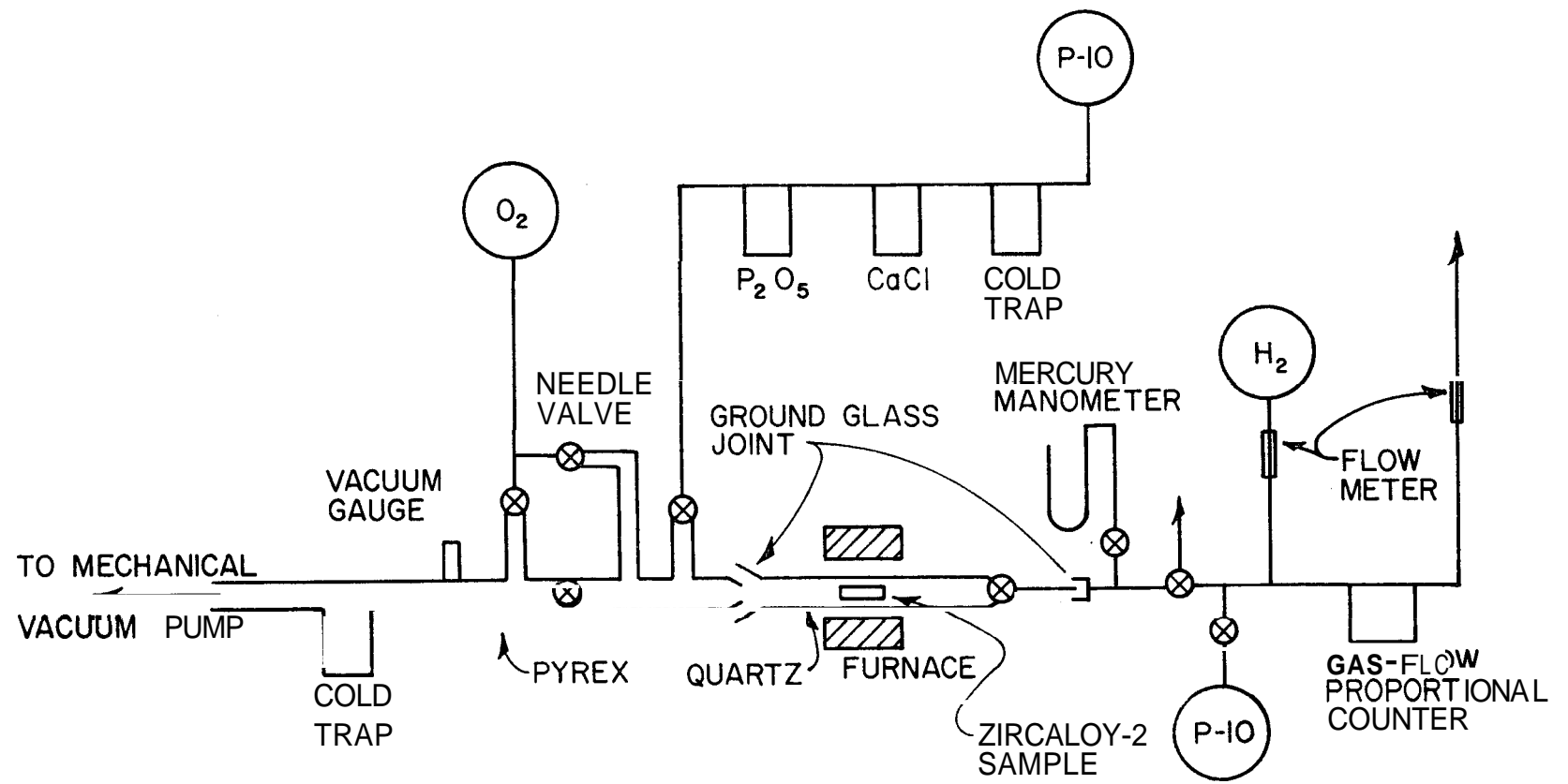
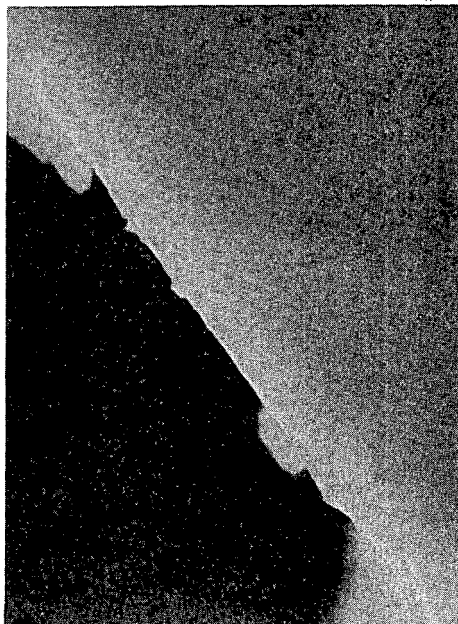
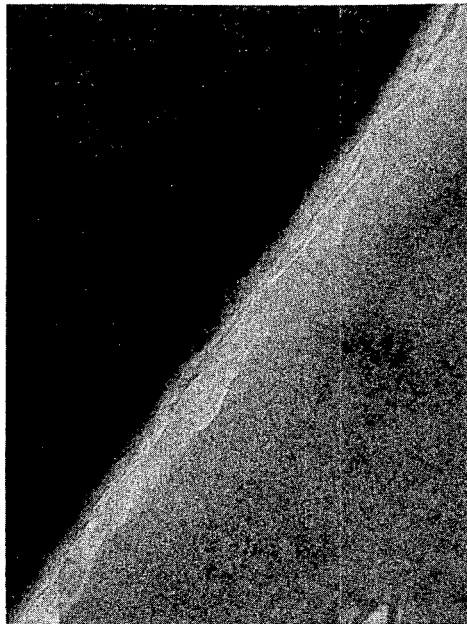


Figure 9. Experimental set-up for oxidation and tritium release studies in Zircaloy

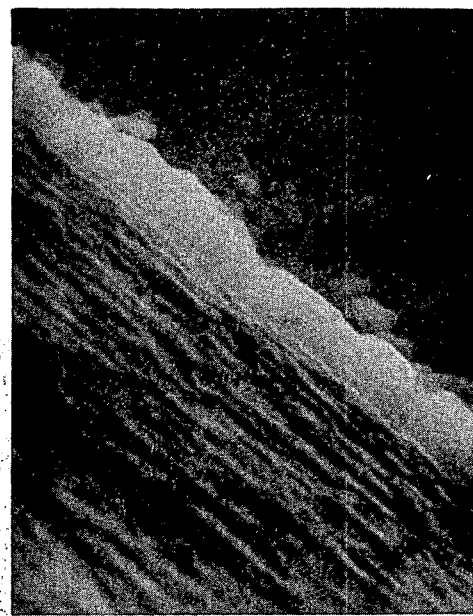
a. Oxidation time 10 min.
(viewed \perp^r to metal surface)



b. Oxidation time 50 min.
(viewed \perp^r to metal surface)



c. Oxidation time 100 min.
(viewed \perp^r to metal surface)



d. Oxidation time 200 min.
(viewed at 18° tilt showing oxide
surface and polished metal surface)

Figure 10. Scanning electron micrographs of oxide films on Zircaloy-2 oxidized at 500°C and 200 Torr. (x 8000)

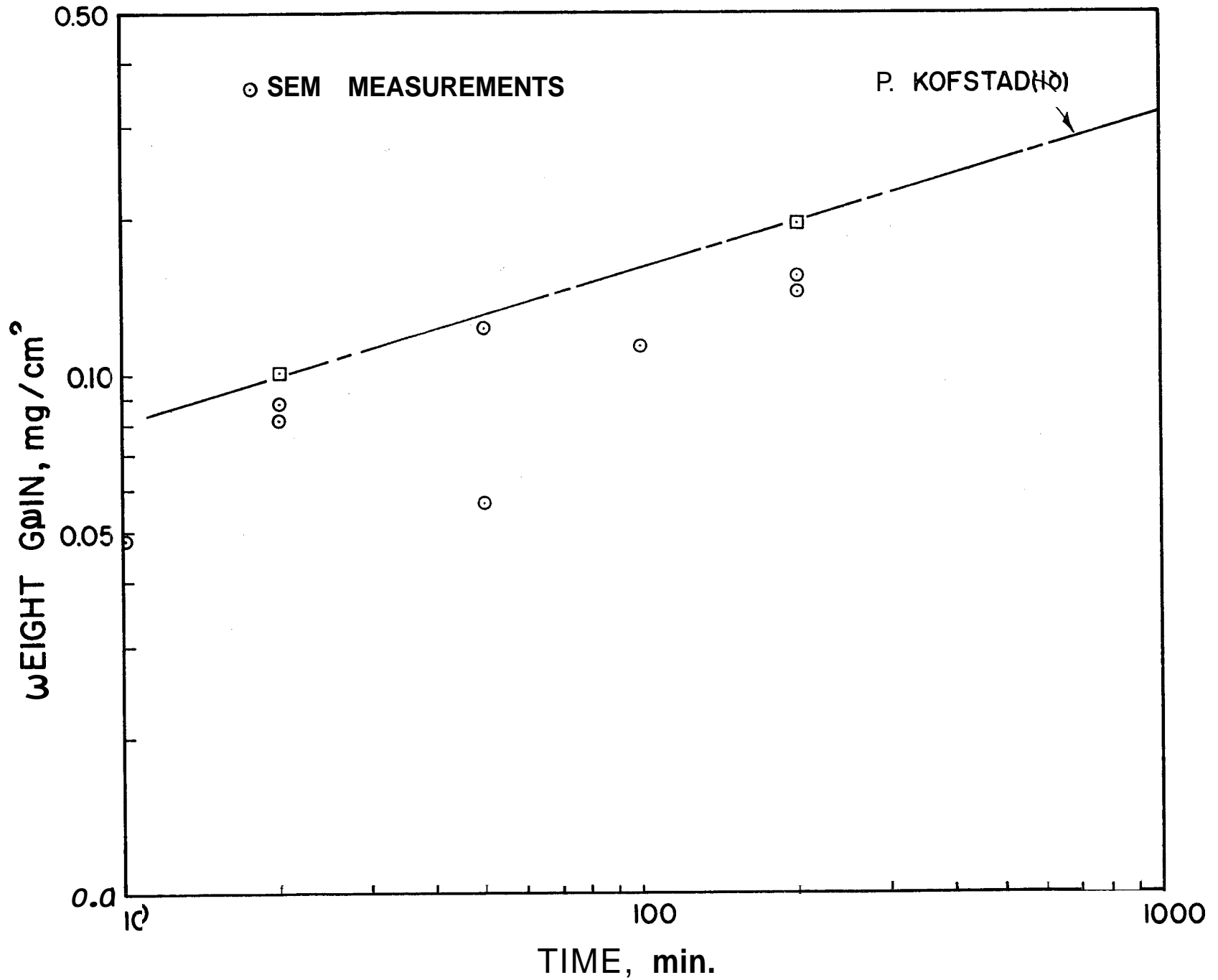


Figure 11. Zircaloy oxide layer thicknesses measured from scanning electron micrographs compared against literature data

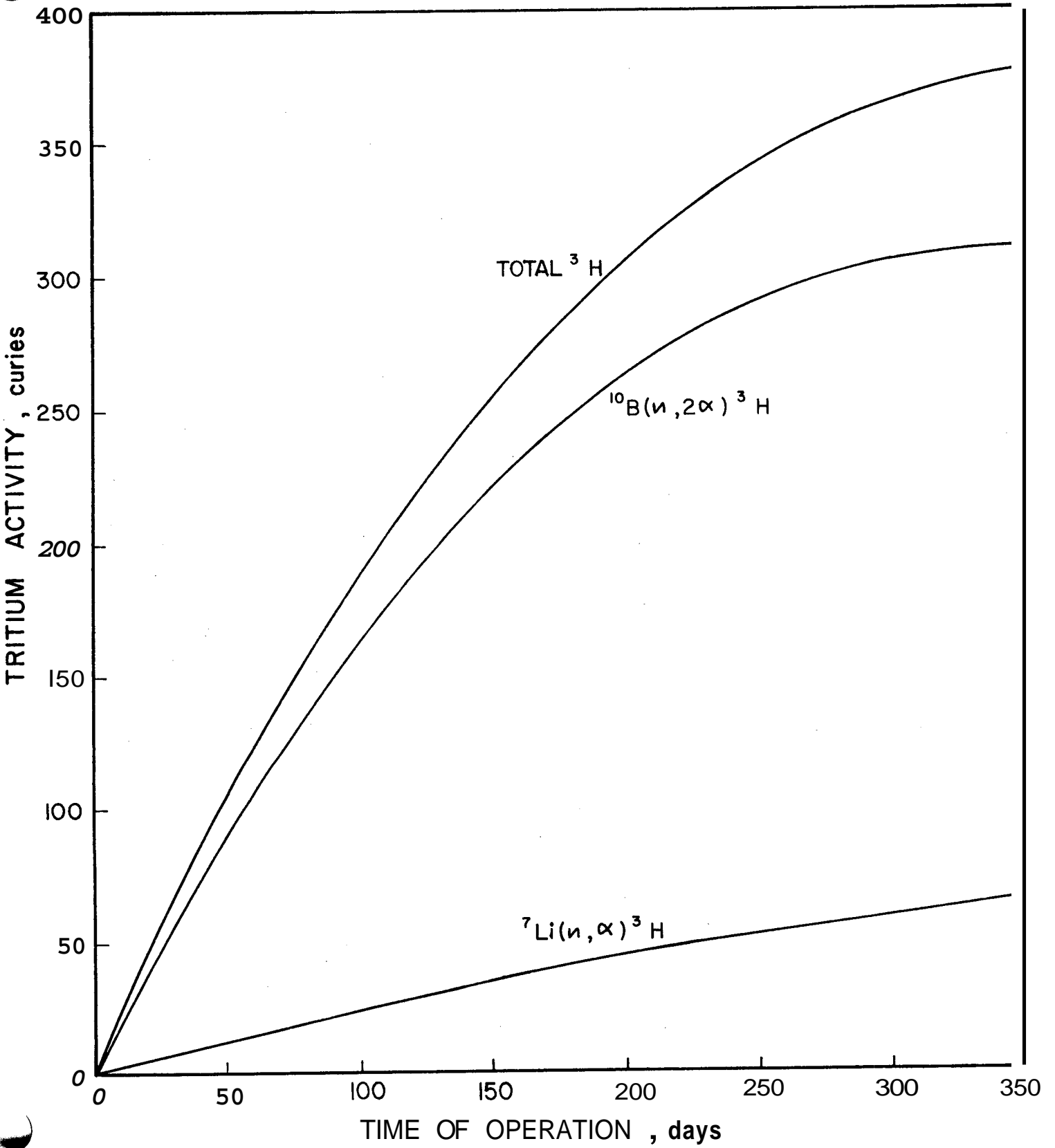


Figure 12. Tritium activity in the primary coolant due to boron and lithium reactions

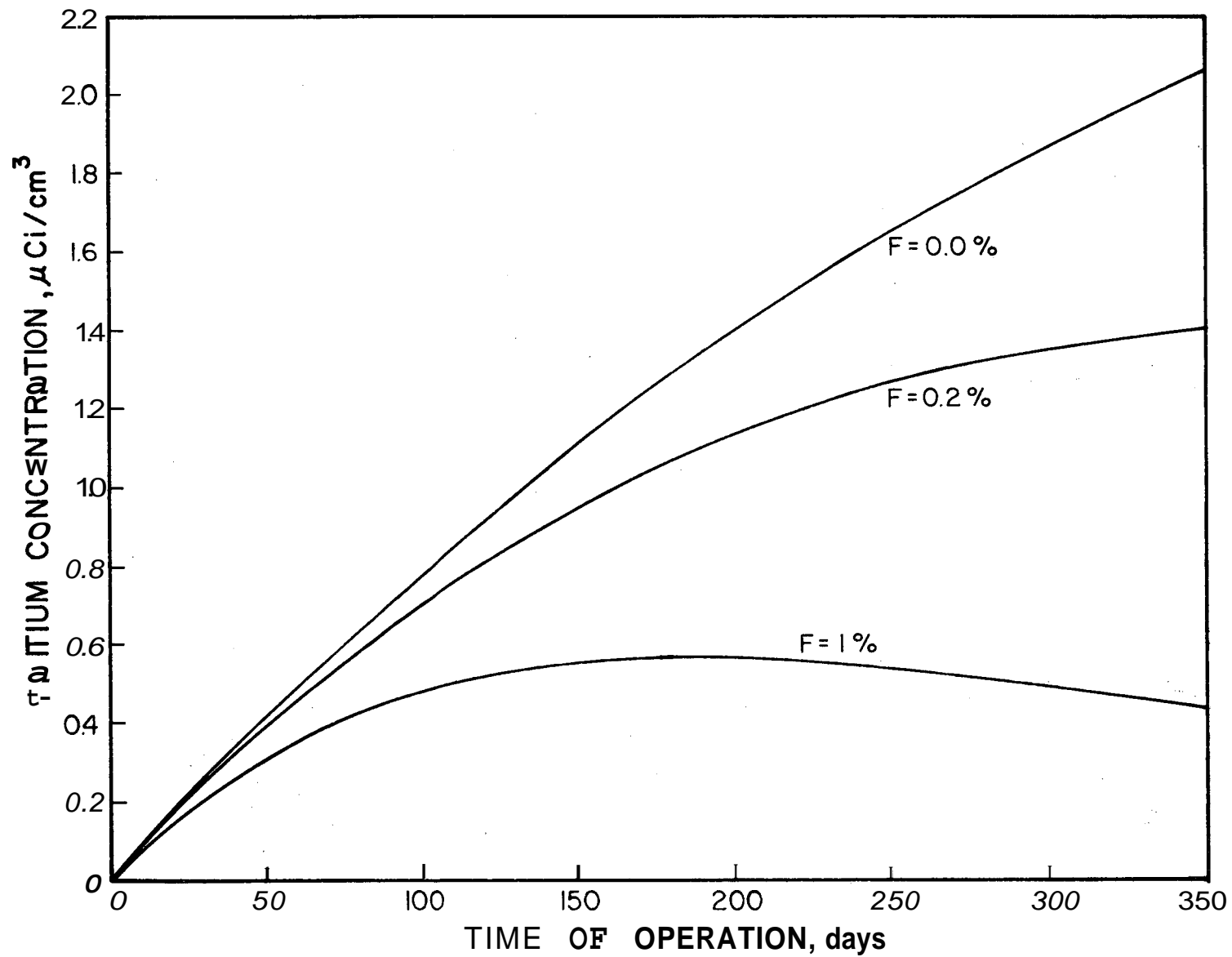


Figure 13. Tritium concentration in the primary coolant for various dilution factors

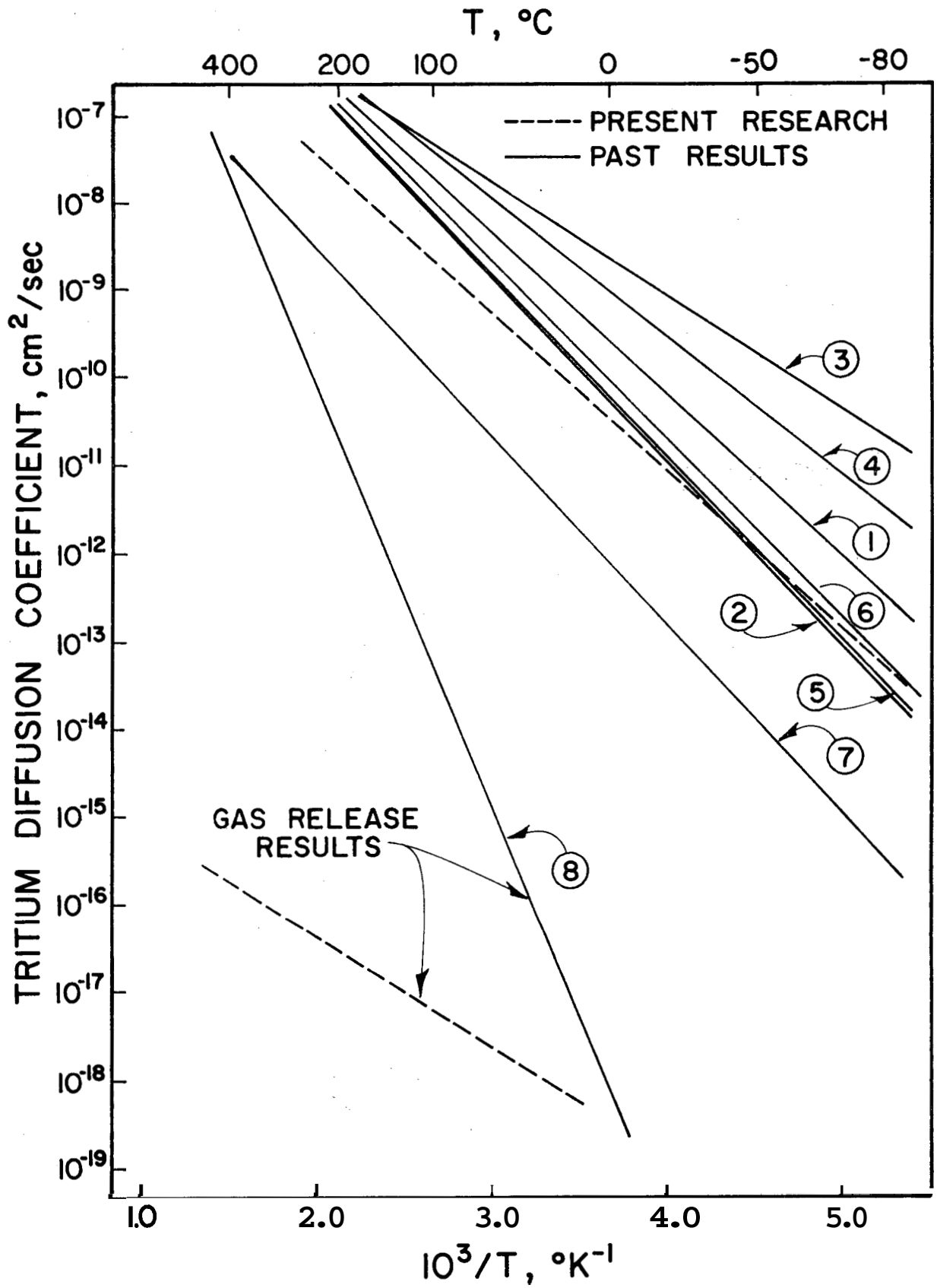


Figure 14. Comparison of Zircaloy diffusion coefficients reported in literature with present work

ANALYSIS OF XENON DIFFUSION DATA USING A TRAPPING MODEL

ABSTRACT

In order to check the extent to which values of xenon diffusion coefficients reported in literature might have been influenced by gas atom trapping, trapping parameters measured in calcium fluoride were modified to suit UO_2 and used in Hurst's trapping model to predict the diffusion coefficients that should have been observed for the experimental conditions used by previous workers. It is shown that a significant fraction of the xenon diffusion coefficients reported in literature for UO_2 is approximately consistent with the classical diffusion coefficient of xenon in UO_2 modified by trapping effects,

INTRODUCTION

Rare gas diffusion studies in solids have been continuing as a part of this project for the past several years. A principal activity has been to better define the relationship between rare gas trapping and post-irradiation gas release experiments with reactor fuel materials. Alkali metal halide and CaF_2 single crystals have been used as substitutes for fissionable materials in order to allow delineation of specific effects. Gas retention in surface films, trapping at radiation-induced defects and gas concentration effects have been identified and studied.

In the recent years the efforts in this direction have been on the measurement of trap concentration and retention time of xenon in the traps in CaF_2 and UO_2 single crystals. These trapping parameters have been determined for four different temperatures in CaF_2 and preliminary measurements have been made at three temperatures in UO_2 . Further the diffusion coefficients in these two materials at low defect concentrations have been measured and in UO_2 values of D were obtained which were higher than most of the diffusion coefficients.

The purpose of the present work is to determine whether or not the trapping parameters measured in CaF_2 and UO_2 could explain quantitatively the wide range of experimental diffusion data quoted in the literature.

SUMMARY OF PREVIOUS WORK

A detailed discussion of the rare gas diffusion experiments and results has been presented in past annual reports and publications. These are:

Annual Progress Report "Effect of Radiation Damage and Gas Concentration, on Rare Gas Diffusion in Solids." USAEC

ORO-3508-1	11/65 to 10/66	} Period Covered by Report
ORO-3508-3	11/66 to 10/67	
ORO-3508-4	11/63 to 10/68	
ORO-3508-5	11/68 to 10/69	
ORO-3508-6	11/69 to 10/70	
ORO-3508-7	11/70 to 10/71	

(Available from: Superintendent of Documents, U. S. Department of Commerce, Washington, D. C.)

"The Diffusion of Recoil Fission Fragments from Solid Surfaces -- Calculated Release Curves," ORO-3508-2 (1967).

"Rare Gas Diffusion in Cesium Iodide -- The Use of Fission Recoil Doping Techniques," J. Amer. Ceram. Soc. 51(10):560-564 (1968).

"Effect of Radiation on Rare Gas Diffusion in Crystals," Trans. Am. Nucl. Soc. 10(2):509 (1967).

"Influence of Defects on Rare Gas Diffusion in Solids," J. Nucl. Mat. 30:89-106 (1969).

"Surface Effects on the Diffusion Release Rate of Rare Gases," Phys. Stat. Sol. (a) 3:921 (1970).

"Effect of Trapping on the Release of Recoil Injected Gases from Solids," Nucl. Instr. and Methods 86:117-125 (1970).

"Rare Gas Diffusion in Alkali Metal Iodides," Phys. Stat. Sol. 7(2) (1971).

"Diffusion and Trapping of Rare Gas Xenon in Calcium Fluoride Single Crystals," J. Nucl. Mat. 42:191-202 (1972).

"Xenon-133 Diffusion and Trapping in Single Crystal UO_2 ," Phy. Stat. Sol. (accepted for publication).

A review of the major results presented in these reports is summarized here as background.

I. Classical Rare Gas Diffusion

The early literature on rare gas diffusion in solids contains surprisingly few examples of classical diffusion behavior. The term, "classical diffusion," is used here to imply a condition where:

1. The time rate of gas release is consistent with solutions to Fick's diffusion equations with constant diffusion coefficient D .
2. The temperature dependence of D is of the general form:

$$D = D_0 e^{-\Delta H/kT}.$$

3. Gas diffusion is controlled by thermally generated defects.

Gas diffusion experiments were carried out for the purpose of establishing whether classical diffusion of a rare gas could be obtained when radiation damage and gas concentration effects were minimized. Single crystals of CsI, RbI, and KI were grown from a melt doped with ^{133}I which is the precursor of radioactive ^{133}Xe . The resulting crystals contained a homogeneous distribution of radioactive rare gas at low concentration with negligible radiation damage to the lattice. Diffusion experiments were performed by isothermally annealing the crystals and radioassaying the released ^{133}Xe as a function of time. The measured gas diffusion coefficients were reproducible and met criteria (1) and (2) for classical diffusion.

Experiments in which ^{133}Xe was recoiled into the surface layers of crystals through fission of an external uranium foil were also employed to study rare gas diffusion. The diffusion coefficients calculated from the back-diffusion of ^{133}Xe from the surface layers of the recoil doped specimens agreed with the values determined from ^{133}I doping as long as fission recoil fluences were kept below approximately 10^{12} fission fragments cm^{-2} . The two experiments were so greatly different that identical results appear justified only if the Xe diffusion is controlled by thermally generated defects in both cases.

The experiments indicate that it is possible to obtain classical diffusion kinetics for rare gas diffusion if radiation damage levels and gas concentrations are low. Table I summarizes the characteristic diffusion coefficients and enthalpies measured for ^{133}Xe diffusion in four solids.

Table I. Measured Diffusion Constants for ^{133}Xe Diffusion in Alkali Metal Iodides and Calcium Fluoride

Solid	D_0 (cm^2/sec)	AH (eV.)	Temperature Range
KI	$1.49^{+3.44}_{-0.84}$	1.03 ± 0.05	150 C - 500 C
RbI	$0.082^{+3.11}_{-0.03}$	0.93 ± 0.05	150 C - 500 C
CsI	$0.57^{+2.30}_{-0.43}$	1.00 ± 0.04	150 C - 500 C
CaF_2	9.5×10^6	4.42	750 C - 1000 C

PI, Gas Atom Trapping in "Growth Induced" Defects

It was found that alkali halide single crystals could be grown which contained considerable strain as the result of defects introduced during the growth process. These crystals were cloudy in appearance and gave indistinct X-ray diffraction patterns, indicative of strain. The defects were presumably small voids and low angle tilt boundaries but no direct observations of the defects were made.

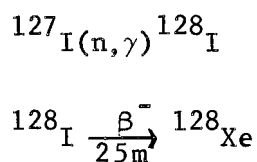
Xenon diffusion measurements on cloudy CsI single crystals gave values for the diffusion coefficient which appeared to decrease with heating time, which was consistent with a trapping process in which gas atoms were being

immobilized at defects while they diffused. Application of the trapping model developed by Hurst⁽¹⁾ showed that the experimental results were consistent with a trap concentration of approximately 1.2×10^{11} traps cm^{-3} and a long retention time in the traps. It was possible to eliminate the traps by annealing the crystals before the ^{133}I decayed to ^{133}Xe and the higher the annealing temperature, the greater the fraction of traps annealed. After the gas atoms become immobilized at the traps, they apparently stabilized the traps as heating at this stage did not result in trap annealing.

III. Gas Atom Trapping at High Gas Concentrations

A series of experiments were carried out to show the effect of gas concentration on rare gas diffusion kinetics. Three types of experiments were performed:

1. Total Xe concentrations were varied by growing alkali halide crystals in a Xe atmosphere with differing Xe partial pressures. The gas tag was introduced through incorporation of ^{133}I into the melt.
2. Total Xe was varied by irradiating alkali halide crystals with different thermal neutron fluences to generate stable ^{128}Xe through the reaction:



The gas tag was again introduced through incorporation of ^{133}I into the melt.

3. Total Xe was controlled by varying the amount of ^{133}I tag added to the alkali halide melt.

The first technique permitted a wide range of Xe concentrations, but it was not possible to insure uniform gas distribution in the solid. Transmission electron microscopy was used to show that at least some of the Xe was inhomogeneously distributed as bubbles. Methods (2) and (3) produced an initially homogeneous gas distribution but they did not permit as wide a range of possible gas concentrations as method (1). Also, some fast neutron radiation damage was produced by (2) even though this was kept to a minimum by irradiating specimens in the reactor thermal column,

Crystals with relatively high rare gas concentrations ($10^{14} - 10^{16}$ atoms cm^{-3}) exhibited lower diffusion coefficients than the crystals with low rare gas concentrations ($10^{10} - 10^{13}$ atoms cm^{-3}), apparently reflecting trapping of gas atoms in small gas clusters or bubbles. Values of D were lowered at all of the studied temperatures for the high concentration cases and the observed D was constant for the gas release at any given temperature.

Flux limitations on our reactor prevented a study of concentration effects over wide concentration limits. However, the experiments do show that rather pronounced effects (an order of magnitude reduction in the observed diffusion coefficient) occurs when gas concentrations are as high as 10 ppm. Experiments with KI single crystals show effects on the diffusion coefficient which appear to result from gas concentration effects at gas concentrations as low as 0.004 ppm. In any event, effects due to gas atom clustering clearly occur in alkali halides in the concentration ranges frequently employed for rare gas diffusion experiments.

IV. Gas Atom Trapping at Radiation-Induced Defects

It was found that radiation produces defects that trap diffusing gas atoms. Radiation damage was produced by doping alkali halide and calcium fluoride crystals through the fission recoil technique at moderately high fission recoil

concentrations ($> 10^{12}$ fission fragments cm^{-2}). Each fission fragment deposited an average of 30 MeV, of which approximately 5% was dissipated in displacement type interactions, so a relatively large fraction of the atoms were displaced. The trapping behavior observed in these crystals differed significantly from the trapping defects produced by high gas concentrations or grown-in defects. The radiation-induced effects annealed at high temperatures, and the best fit of the trapping model to the experimental data showed that the trap concentrations were considerably higher and the mean gas retention time in traps considerably lower than was observed with the crystals containing growth-generated defects. The radiation-induced traps had a concentration of at least 10^6 higher than the traps produced by growing defective crystals. Annealing of the radiation-induced defects was not affected by gas stabilization of the traps since the trap concentrations exceeded the gas concentrations.

A detailed analysis was carried out of the trap concentrations and retention times in traps for fission doped CaF_2 single crystals. The model proposed by Hurst⁽¹⁾ was modified for use with fission recoil gas concentration profiles, and trap concentrations and gas retention times were calculated from gas release experiments conducted at two concentrations and four temperatures. The trap concentrations were found to be too high to be explained in terms of gas atom clustering and must have resulted from radiation damage. Semi-log plots of trap concentrations and trap retention times versus $(\text{temperature})^{-1}$ gave straight lines, implying that these quantities were adequately represented by single values for the activation energies over the temperature range studied.

The experiments summarized in Sections II, III, and IV indicate three distinct gas atom trapping processes which can occur in solids -- trapping at small voids and other defects produced during crystal growth, trapping

through gas atom clustering at high gas concentrations, and trapping at radiation-induced defects. Each trapping process led to somewhat different gas release kinetics and a different temperature dependence for diffusion,

V. Mechanism of Gas Diffusion

The classical diffusion results were interpreted in terms of possible gas diffusion mechanisms. The two most well-established diffusion processes, interstitial diffusion and vacancy diffusion, are incompatible with much of the available data on rare gas migration, including the results of the present study. The principal objection to an interstitial mechanism is the wide discrepancy between calculated and observed diffusion activation energies with the observed values greatly exceeding the calculated values. This discrepancy was supported by the present study where the measured diffusion activation energies for Xe diffusion in KI, RbI and CsI were observed to be approximately three times the calculated migration energies for interstitial diffusion⁽²⁾.

Objections to simple vacancy diffusion are based upon the absence of an impurity effect on the observed diffusion coefficient⁽³⁻⁶⁾, channeling results with alpha-emitting rare gases^(7,8), and the wide discrepancy between rare gas diffusion results and self-diffusion results where self-diffusion is known to occur by a vacancy mechanism⁽⁹⁾. The present work has noted the absence of an impurity effect for Xe diffusion in Cu_2O and BaI_2 doped crystals and the large difference between the Xe and self-diffusion coefficients.

The two mechanisms that are most frequently discussed as applicable to rare gas diffusion are the trapped-interstitial model proposed by Norgett and Lidiard⁽¹⁰⁾ and the mobile defect cluster model first suggested by Matzke⁽¹¹⁾. The trapped-interstitial model assumes that rare gas atoms diffuse interstitially but that they also become trapped at defects such as vacancies. The release rate from the vacancy traps can be the rate-

determining step in gas diffusion under certain conditions and the measured diffusion activation energy will therefore be higher: than that predicted for interstitial migration. The mobile defect cluster model assumes that gas atoms associate with mobile defect clusters in the lattice and move with these clusters through the lattice,

The principal inconsistency between the trapped-interstitial diffusion model and the present work lies in the fact that unusually high defect concentrations are required to explain the low temperature, fission recoil diffusion results where the gas atoms move extremely short distances before release at a surface. The mobile cluster model appears qualitatively consistent with the experimental results and it appears to be the better choice of the two to explain rate gas diffusion in alkali halides.

VI. Diffusion and Trapping in UO₂ Single Crystals

Diffusion studies were performed with UO₂ single crystals using fission-recoil doping and radioassay of the released ¹³³Xe. It was observed that below a fission fragment dose of 3×10^{11} ff cm⁻², classical diffusion solutions would fit the gas release, implying that radiation induced defects did not affect the diffusion process. The classical diffusion coefficient could be represented by

$$D = 2.88 \times 10^3 \exp(-4.78 \pm 110 \text{ Cals/kT}) \text{ cm}^2 \text{ sec}^{-1}$$

over the temperature range 1065°C to 1300°C. Increasing the recoil concentration to 3×10^{12} fission fragments/cm² (3×10^{-8} fission atom fraction) produced anomalies in the gas release curves which probably resulted from gas atom trapping. The gas release curves at this fission fragment dose were consistent with the trapping model of Ong and Elleman⁽¹²⁾. The trap concentrations and retention time in the traps could be determined at 3×10^{12} fission fragments/cm² at three different temperatures.

CURRENT RESULTS AND DISCUSSION

Figure 1 shows Arrhenius plots of diffusion coefficients of Xenon in UO_2 reported by thirteen independent investigations and selected on the basis of clarity of description of the experimental conditions and specimen characterization. The references to each set of data is shown on the page following Figure 1. The eight orders of magnitude spread in these results appears to result principally from the combined effects of trapping in internal pores, trapping at radiation induced defects and uncertainty in the interpretation of non-classical gas release kinetics. In certain selected cases, hyperstoichiometry, impurity effects and faulty surface measurements may also contribute to the spread in the results. It is of interest to determine the extent to which the spread in the diffusion coefficients can be explained solely in terms of trapping at radiation-induced defects since this has been identified in UO_2 as well as in other solids as a major source of error in diffusion studies.

MacEwan and Morel⁽¹³⁾ and Spindler and Lindner⁽¹⁴⁾ have measured values of these trapping parameters for UO_2 . However, their results as well as those of Carter⁽¹⁵⁾ cover only isolated conditions and it is not possible to determine a clear pattern for either the trap concentrations or gas retention times. Ong and Elleman⁽¹⁶⁾ have carried out more extensive measurements of trapping for ^{133}Xe diffusion in single-crystal CaF_2 at several fission fragment concentrations and were able to represent trap concentrations and average retention times for gas atoms in traps as exponential functions of temperature for a given recoil concentration.

CaF_2 has often been used as a model substitute for UO_2 in diffusion studies because of the similarity of the two materials in their physical structure and in the activation energies for rare gas diffusion. Therefore, it was decided to generate the trapping parameters for UO_2 from the

results of Ong and Elleman⁽¹⁶⁾ for CaF_2 . It would seem reasonable to assume that CaF_2 and UO_2 could exhibit identical trapping behavior at equivalent reduced temperatures based on their melting points. So the approach used in this work has been to generate trap concentrations, $[T]$, and retention times, τ_2 , in CaF_2 as a function of fission mole fractions in CaF_2 for various temperatures. For a known fission density and temperature in UO_2 at which a particular published experiment was conducted, the corresponding values of $[T]$ and τ_2 can be determined. From these values and the classical diffusion coefficients quoted for UO_2 by Carter, Driscoll and Elleman^{''''}, and using Hurst's trapping model⁽¹⁾, the diffusion coefficient that a particular author would have obtained if his data were influenced by trapping can be calculated and compared against the value quoted by the author.

Figures 2 and 3 show the curves of $[T]$ and τ_2 as a function of fission mole fraction (FMF) in CaF_2 for a range of temperatures which cover the experiments reported in literature. These curves were generated from the data for CaF_2 reported by Ong and Elleman⁽¹⁶⁾.

According to the Hurst model^{''''}, if an equilibrium is rapidly established between trapping and release from traps, then the observed value of the diffusion coefficient can be represented as

$$D_{\text{obs}} = \frac{1}{(1+k)} D_{\text{true}} \quad (1)$$

where

$$k = \frac{d^2}{3D_{\text{true}}[T]\tau_2} \quad (2)$$

and D_{true} = true diffusion coefficient in UO_2 .

D_{true} in this calculation is taken to be values quoted by Carter, Driscoll and Elleman⁽¹⁵⁾.

In order to perform this calculation with respect to previously published experiments on UO_2 , seven different authors were selected from

the thirteen shown in Figure 1. The ones that reported the lowest values of D were selected since these were thought to be most influenced by trapping. These results are represented by curves labelled (1), (29), (4), (59), (6), (10A), (10B), and (12). From the fission densities and temperatures quoted by the authors, $[T]$ and τ_2 were determined using Figures (2) and (3). These values were substituted into equations (1) and (2) and D_{obs} were determined,

Figure (4) shows these values compared against the values reported by these authors. Although the spread in the results is reduced by this trapping model, it gives values of D which are several orders of magnitude below the corresponding reported results. Because of the uncertainties about what portion of the gas release curves were used by the various authors in determining their values of diffusion coefficients, one would not expect a fit of the values calculated by the trapping model with the experimental values to better than a couple of orders of magnitude.

The trapping parameters of Ong and Elleman⁽¹⁶⁾ for CaF_2 differed by several orders of magnitude from the values of MacEwan and Morel⁽¹³⁾ and of Spindler and Lindner⁽¹⁴⁾ for UO_2 at equivalent reduced temperatures. An arbitrary displacement of the CaF_2 trapping results parallel to the temperature axis was made to provide closer agreement between the two sets of data. There is no fundamental justification for this adjustment, except the recognition that it is unrealistic to expect exact correspondence between UO_2 and CaF_2 and it is probably best to ascribe the greatest reliability to the few direct measurements which have been carried out for UO_2 . The other essential features of the CaF_2 trapping values such as temperature and fission density dependence were retained unaltered.

Figure (5) shows the D_{obs} calculated using these adjusted trapping parameters and they are in reasonable agreement with the values reported by the authors. Of the 52 values checked for a variety of temperatures

and fission densities, the agreement between the calculated and measured values agreed to within an order of magnitude for two-thirds of the cases and differed by more than two orders of magnitude for only four points.

In several cases, where there was disagreement between calculated and experimental diffusion coefficients, it was apparent that different values of the diffusion coefficient could be inferred from the curves generated by Hurst's model, depending on which portion of the curve was selected for fitting to the classical diffusion solutions. The range of possible diffusion coefficients often included the literature reported value for the selected temperature and fission density. In other cases, it was found that the literature value of D could be obtained by varying either the trap concentration or gas retention time by no more than a factor of ten, a variation which is clearly possible in view of the uncertainties involved in estimating the trapping parameters.

CONCLUSIONS

The principal conclusion which can be made from these results is that trapping at radiation-induced defects in UO_2 is a probable cause of most of the discrepancies observed in rare gas diffusion coefficients that are reported in literature. The fact that trapping parameters measured for CaF_2 and adjusted to correspond with the limited trapping data available in UO_2 could give observed diffusion coefficients in agreement with a number of literature values lends support to this conclusion.

A more accurate analysis of trapping would necessitate measurement of rare gas trapping parameters in UO_2 over a wide range of fission densities and temperatures.

REFERENCES

1. Hurst, D. G., "Diffusion of Fission Gas: Calculated Diffusion from a Sphere Taking Into Account Trapping and Return from the Traps," CRRP-1124, Atomic Energy of Canada, Ltd., Chalk River, Ontario, Canada (1962).
2. Norgett, M. J. and A. B. Lidiard, "The Migration of Inert Gases in Ionic Crystals," Phil. Mag. 18:1193-1210 (1968).
3. Matzke, HJ., "Rare Gas Mobility in Pure and Doped Potassium Bromide," Z. Naturforsch. 22a:507-518 (1967).
4. Matzke, HJ., D. Rickers, and G. Sorenson, "Rare Gas Diffusion in NaCl," Z. Naturforsch. 24a:820-826 (1969).
5. Ong, A. S., "The Diffusion of ^{133}Xe in CsI and CaF_2 Single Crystals," M.S. Thesis, North Carolina State University, Raleigh, North Carolina (1970); Also ORO-3508-3 (1967).
6. Matzke, HJ., "Xenon Migration and Trapping in Doped ThO_2 ," J. Nucl. Mat. 21:190-198 (1967).
7. Matzke, HJ., "Application of 'Channeling' Techniques to Fission Gas Release Studies," J. Nucl. Mat. 30:110-121 (1969).
8. Matzke, HJ., and J. A. Davis, "Location of Inert Gas Atoms in KCl, CaF_2 and UO_2 Crystals by H^+ and He^{2+} Channeling Studies," J. Appl. Phys. 38(2):805-808 (1967).
9. Elleman, T. S., C. H. Fox, Jr., and L. D. Mears, "Influence of Defects on Rare Gas Diffusion in Solids," J. Nucl. Mat. 30:89-106 (1969).
10. Norgett, M. J. and A. B. Lidiard, "The Migration of Inert Gases in Ionic Crystals," Phil. Mag. 18:1193-1210 (1968); Also, Harwell Report, TP332 and 370.
11. Matzke, HJ., "Rare Gas Mobility in Pure and Doped Potassium Bromide," Z. Naturforsch. 22a:507-508 (1967).
12. Ong, A. S., and T. S. Elleman, "Effect of Trapping on the Release of Recoil Injected Gases and Solids," Nucl. Instr. and Methods, 86: 117-125 (1970).
13. MacEwan, J. R., and P. A. Morel, "Migration of Xenon through a UO Matrix Containing Trapping Sites," Nucl. Appl. 2:158-170 (1966).
14. Spindler, P. and R. Lindner, "Diffusion of Xenon-133 in UO_2 Single Crystals," Z. Naturforsch. 21a:1723-1725 (1966).
15. Carter, J. C., "Rare Gas Diffusion in UO_2 Single Crystals Using Fission Recoil Doping Techniques," M. S. Thesis, Department of Nuclear Engineering, North Carolina State University, Raleigh, North Carolina (1971).

16. Ong, A. S., and T. S. Elleman, "Diffusion and Trapping of Rare Gas Xenon in Calcium Fluoride **single** Crystals," Jour, Nucl. Mat. 42:191-202 (1972).
17. carter, J. C., E. J. Driscoll, and T. S. Elleman, "Xenon-133 Diffusion and Trapping in **single** Crystals Uranium Di Oxide," Phys. Stat. Solidi. (in press).

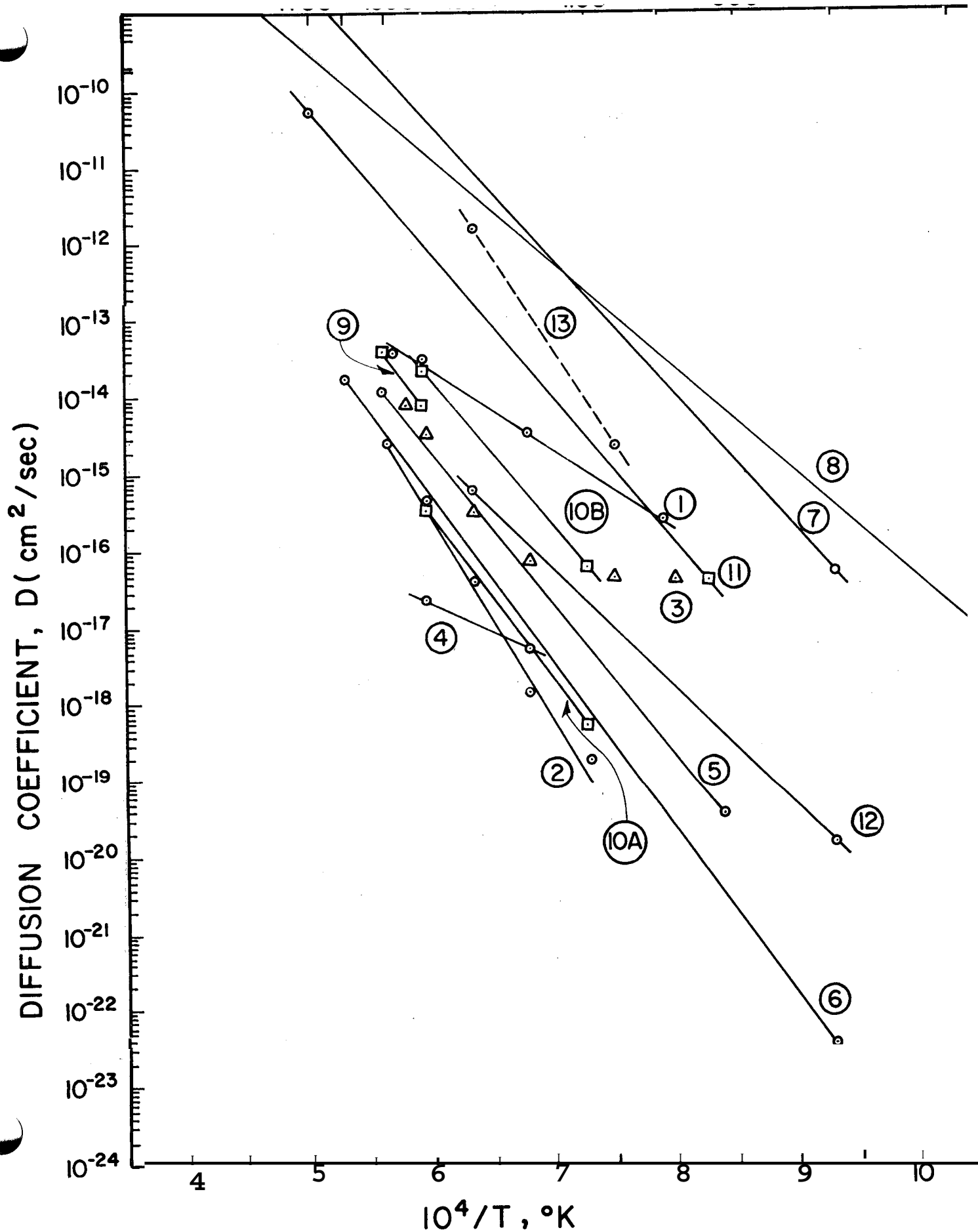


Figure 1. Arrhenius plots of diffusion coefficient of xenon in uranium dioxide reported in literature

References to Figure 1

- | | |
|--|--|
| 1. Booth and Rymer (1958) Fused UO_2 | $D = 1.5 \times 10^{-8} \exp(-46,000/RT)$ |
| 2. Stevens and MacEwan (1960) Fused Oxide | $D = 2.4 \exp(-120,000/RT)$ |
| 3. Auskern (1960) Crushed UO_2 | $D = 2.6 \times 10^{-4} \exp(-65,500/RT)$ |
| 4. Barnes, <u>et al.</u> (1961) Single Crystal | $D = 1.39 \times 10^{-3} \exp(-30,200/RT)$ |
| 5. Melehan, <u>et al.</u> (1963) Sinter | $D = 2 \times 10^{-3} \exp(-92,000/RT)$ |
| 6. Davies and Long (1963) Single Crystal | $D = 9.3 \times 10^{-3} \exp(-100,000/RT)$ |
| 7. Soulhier and Schuremkamper (1964)
Single Crystal | $D = 2.8 \exp(-82,000/RT)$ |
| 8. Oi (1965) Single Crystal | $D = 3 \times 10^{-3} \exp(-63,000/RT)$ |
| 9. MacEwan and Morel (1966)
Single Crystal | |
| 10. Spindler and Lindner (1966)
Single Crystal | (A.) $D = 1.6 \times 10^{-3} \exp(-96,800/RT)$
(B.) $D = 5.5 \times 10^{-3} \exp(-87,300/RT)$ |
| 11. Felix (1970) Fused UO_2 | $D = 5 \times 10^{-1} \exp(-89,834/RT)$ |
| 12. Belle, <u>et al.</u> (1960) Powder | $D = 6.6 \times 10^{-6} \exp(-71,700/RT)$ |
| 13. Carter (1971) Single Crystal | $D = 2.88 \times 10^{-3} \exp(-110,227/RT)$ |

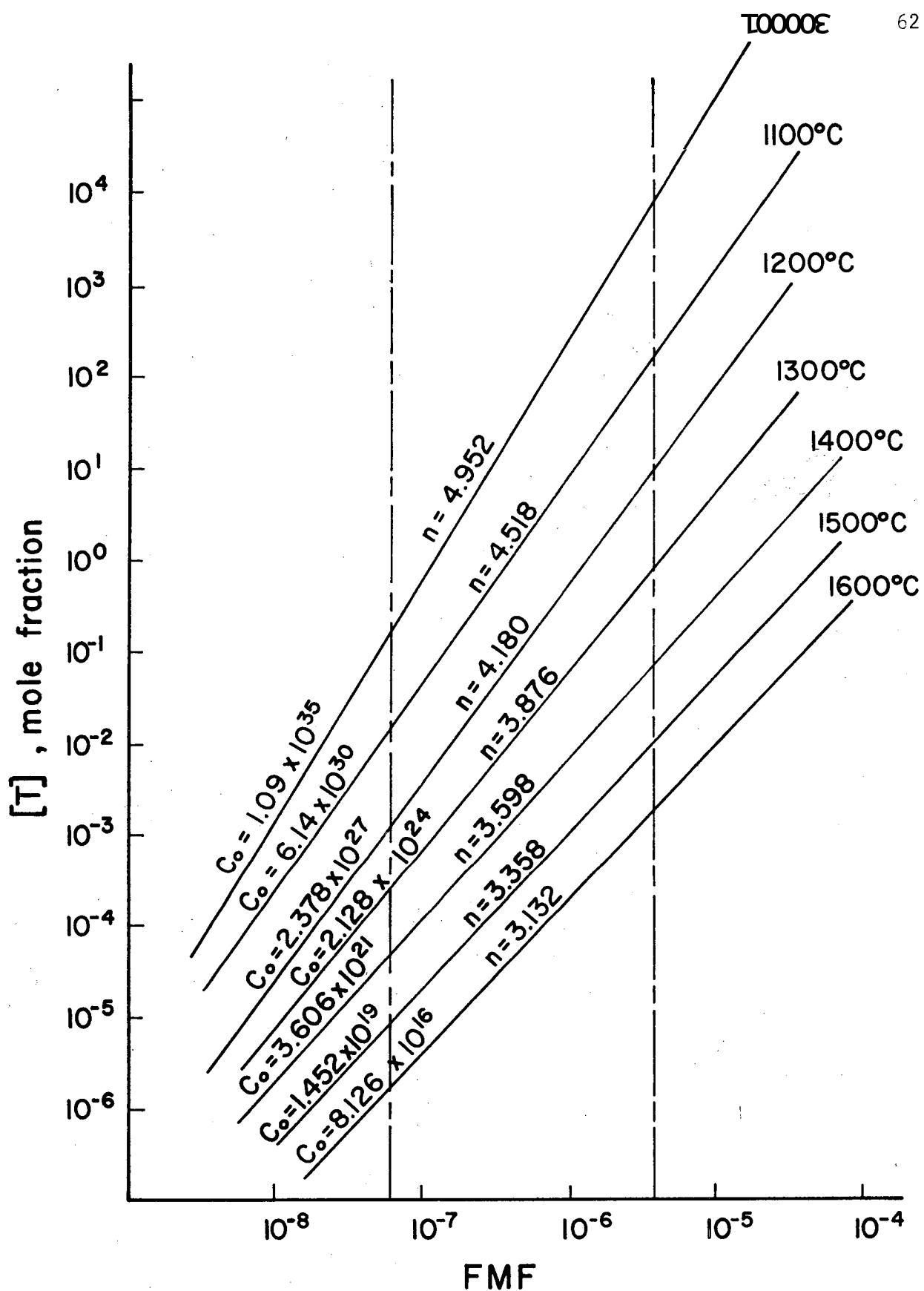


Figure 2. Trap concentration as a function of fission mole fractions in CaF_2 $[T] = C_0 [\text{FMF}]^n$

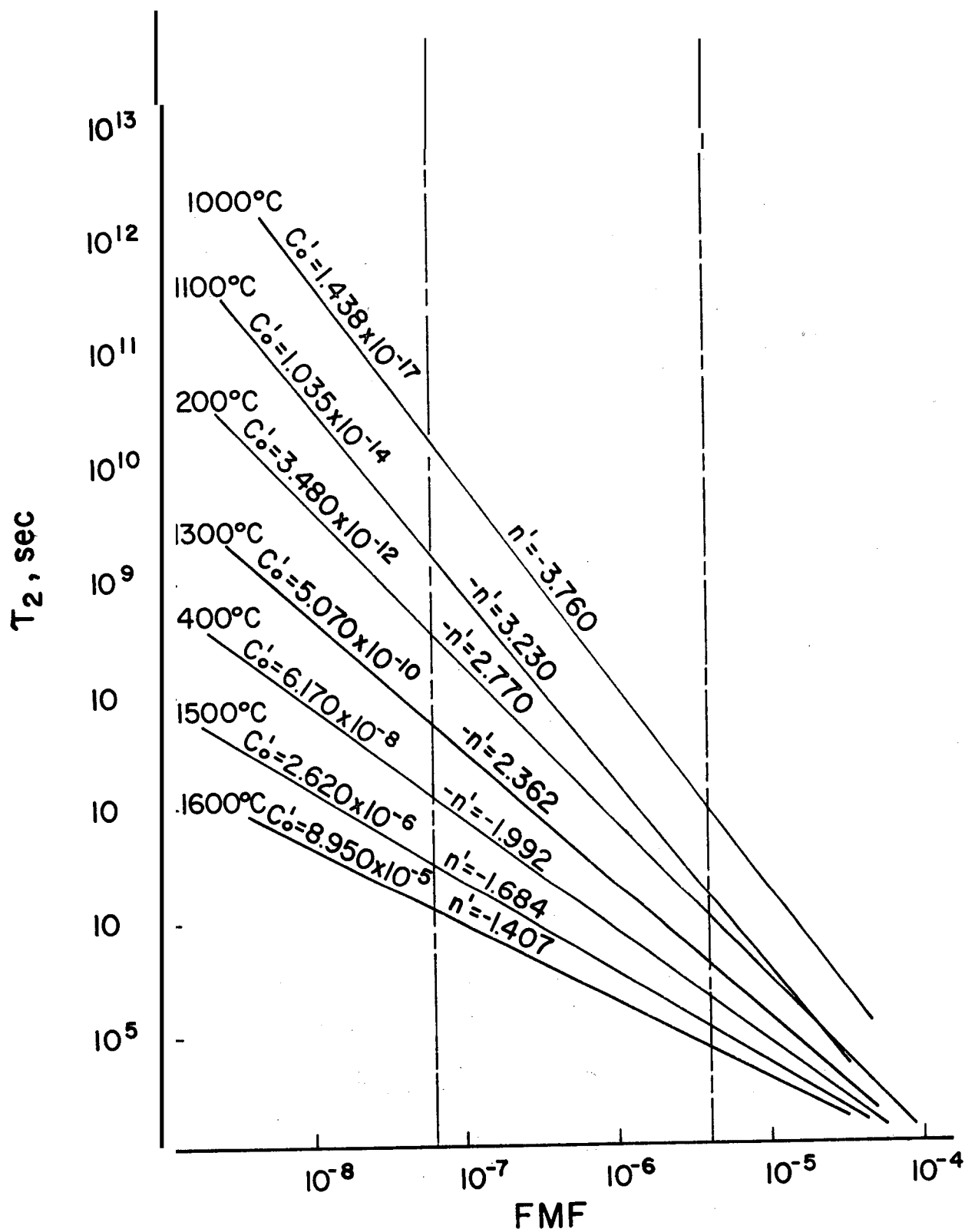


Figure 3. Retention time in the traps as a function of fission mole fractions in CaF_2 $\tau = C_0' [\text{FMF}]^{-n}$

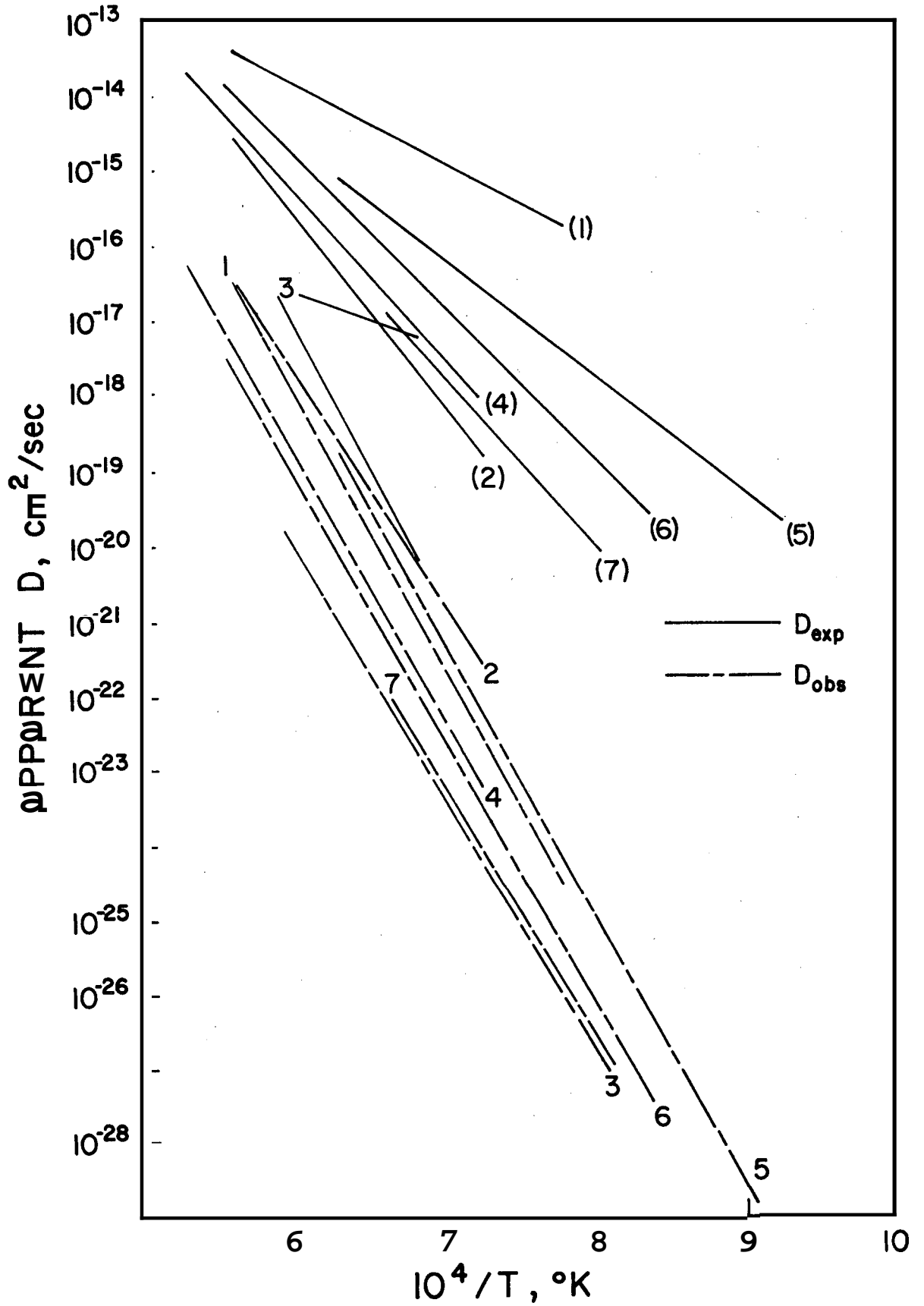


Figure 4. Calculated D using the trapping model compared against: the experimental values

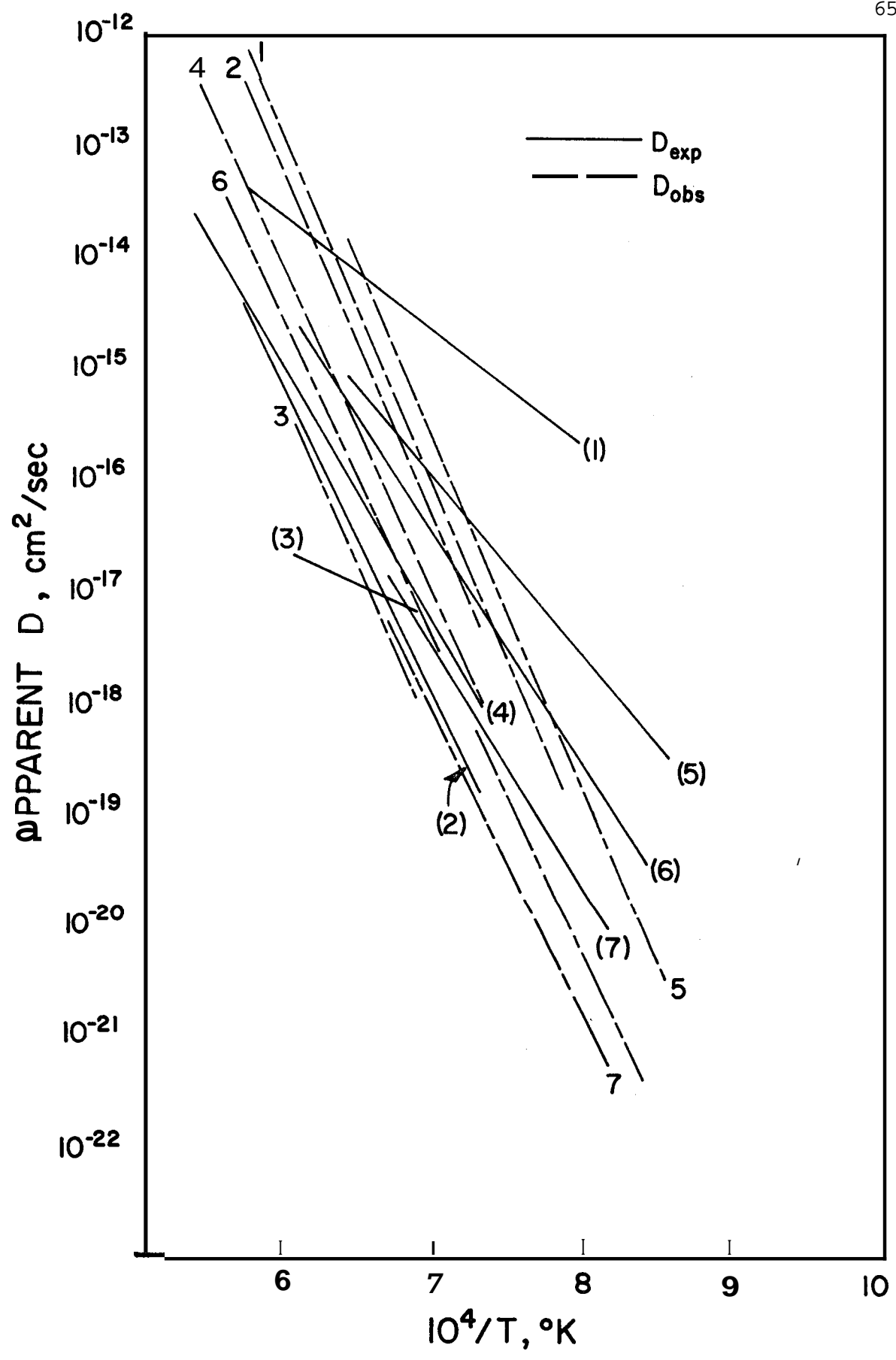


Figure 5. Values of D calculated by the trapping model and adjusted trap parameters compared against literature values